# Development of a parameter for combustion noise control

Senbaha Karthikeyan, Chandrabalan

Master of Science Thesis MMK 2012:70 MFM 151

KTH Industrial Engineering and Management

Machine Design

SE-100 44 STOCKHOLM

KTH Industriell teknik och management

**Examensarbete MMK 2012:70 MFM 151**

# Development of a parameter for combustion noise control

Senbaha Karthikeyan,Chandrabalan

| Godkänt | Examinator | Handledare |
|---|---|---|
| 2012-Sep-25 | Andreas Cronjhort | Andreas Cronjhort |
| | Uppdragsgivare | Kontaktperson |
| | Thorsten Schnorbus,Aachen | Joschka Schaub |

## *Sammanfattning*

De ständigt ökande kraven från emissionslagstiftningen har gjort att fordonsindustrins huvudfokus har riktats mot att minska utsläppen från koldioxid (CO2) och bildandet av andra föroreningar från nya motorer. Ett resultat av detta är att flera motortillverkare har valt nya tekniksp˚ar som ofta leder till ökat motorbuller vilket är ofördelaktigt tillsammans med dieselmotorns karaktäristiska redan höga förbränningsljud. Exempelvis leder ”downsizing” till att motorns belastning ökar vilket i sin tur ger ökat motorbuller. I detta examensarbete har en undersökning för att identifiera lämpliga parametrar som kan förutsäga förbränningsljud utförts. Utredningen har fokuserat på olika parametrars noggrannhet associerade med förbränningsljud vid olika motorkörfall. Lämpliga parametrar inkluderades i ett Rapid Control Prototyping (RCP) system och verifierades genom att använda mikrofoninspelning på en akustisk chassidynamometer. Utredningen visar att maximal grad av värmefrigivning över tid överensstämmer bra med förbränningsljud vid olika körfall. Detta kunde också påvisas med resultaten av ljudupptagningarna från den akustiska chassidynamometern.

KTH Industrial Engineering and Management

**Master of Science Thesis MMK 2012:70 MFM 151**

**Development of a parameter for combustion noise control**

Senbaha Karthikeyan, Chandrabalan

| Approved | Examiner | Supervisor |
|---|---|---|
| 2012-Sep-25 | Andreas Cronjhort | Andreas Cronjhort |
| | Commissioner | Contact person |
| | Thorsten Schnorbus, Aachen | Joschka Schaub |

# *Abstract*

Ever increasing demand from the legislative requirements has shifted the focus of Automotive Engineering Industries on reducing the overall carbon dioxide ($CO_2$) from the vehicle and reducing the pollutant formation at source. This result in many engine manufacturers opting for new technologies, often these technologies results in an adverse effect on noise adding to the inherent characteristic noise of diesel engines. For example, downsizing the engine results in increase of mean operating load resulting in increased noise. In this thesis work, an investigation for identifying a suitable parameter for predicting combustion noise is performed. The work investigates different parameters associated with combustion noise for its accuracy at various engine operating conditions. Then suitable parameters are implemented on a Rapid Control Prototyping (RCP) system and verified using microphone recording on an acoustic chassis dynamometer. The outcome of the study suggest that maximum rate of heat release with respect to time correlates well to the combustion noise at different operating conditions, it is also verified using the microphone data measured on acoustic chassis dynamometer.

# NOMENCLATURE

*Here are the Notations and Abbreviations that are used in this Master thesis.*

## Notations

| Symbol | Description |
|---|---|
| $P_{max}$ | Maximum Pressure |
| $\alpha_{Pmax}$ | Crank angle at which maximum pressure occurs |
| $dP/d\alpha_{max}$ | Maximum rate of pressure rise with respect to Crank angle |
| $dP/dt_{max}$ | Maximum rate of pressure rise with respect to time |
| $\alpha_{dP/dtmax}$ | Angle at which maximum rate of pressure rise occurs |
| $dQ/d\alpha_{max}$ | Maximum rate of heat release with respect to Crank angle |
| $dQ/dt_{max}$ | Maximum rate of heat release with respect to time |
| $\alpha_{dQ/dtmax}$ | Angle at which maximum rate of heat release occurs |
| $t_i$ | Ignition delay |
| $dP/dt_{max})/t_i$ | Combined parameter 1 |
| $dP/dt_{max})\ ^2(P_{max})^{0.5}/t_i^2$ | Combined parameter 2 |
| $\kappa$ | Expansion co-efficient |
| $dV$ | Change in volume |
| $V_s$ | Swept volume |
| $C_v$ | Specific heat capacity at constant volume |
| $C_p$ | Specific heat capacity at constant pressure |
| $R$ | Universal gas constant |

# *Abbreviations*

| | |
|---|---|
| *$CO_2$* | *Carbon-di-oxide* |
| *EGR* | *Exhaust Gas Recirculation* |
| *CSL* | *Combustion Sound Level* |
| *CNL* | *Combustion Noise Level* |
| *BMEP* | *Brake mean effective pressure* |
| *PMEP* | *Pumping mean effective pressure* |
| *IMEP* | *Indicated mean effective pressure* |
| *RCP* | *Rapid Control Prototyping* |
| *SOC* | *Start of Combustion* |
| *EEOC* | *Estimated End of Combustion* |
| *E-VI* | *European Emission Legislation* |
| *ECU* | *Electronic Control Unit* |
| *MFB* | *Mass Fraction Burned* |

# TABLE OF CONTENTS

# 1 INTRODUCTION

With the introduction of $CO_2$ regulations from the vehicle with the upcoming E-VI emission norms, automotive manufacturers are trying a lot of new technologies and methods to meet these legislative demands without compensating for emission and ever increasing customer expectations. One of the major objectives is to improve the combustion thereby reducing the emission at source and improve the fuel economy. For diesel engines, the trend is more towards downsizing the engine and increase in the power output. Various features such as variable valve timing, two stage turbocharging with intercooler, split engine cooling with on-demand electric water pump, dual loop EGR are finding its way to the passenger car diesel engine segment. The development of low-cost cylinder pressure sensors has promoted closed loop combustion control based on cylinder pressure information in diesel engines [1]. Modern fuel injection equipments are capable of injecting fuel at higher pressures and are coming with optimized layout of the injector nozzle.

Along with the introduction of these new technologies to satisfy the legal requirements, there is a huge demand from the customers on the comfort level of the vehicle and reduction of noise from the vehicle. Several methodologies and improvements in design were introduced to filter the noise from the engine compartment to the driver cabin. There is a significant contribution from the combustion noise to the overall vehicle noise level at start and warm-up conditions and during low speed and low load operation. Inherent noise from the diesel engine combustion is reduced by design changes to the combustion process, mostly by optimizing the calibration parameters of the engine with optimum pilot, rail pressure, boost pressure etc. There is a need to reduce the combustion noise at source without degrading the fuel economy and emission. In order to optimize the combustion noise at source, the combustion noise or the overall noise from the engine must be predicted during engine operation.

There are several methods which can predict combustion noise or overall noise from the engine using the cylinder pressure traces or other equivalent technologies like AVL noise meter. The existing noise algorithms that predicts combustion noise from cylinder pressure traces are often complex and require lot of computational power. There is a necessity to predict combustion noise by using a simple parameter that can be used in real time at low

computational power on a state of the art ECU. This parameter can then be used in closed loop control to control the combustion noise.

# 2 OBJECTIVE

*This chapter presents the objectives and limitations of the current work.*

The major objective is to develop a parameter for predicting combustion noise. The current thesis work involves study of different cylinder pressure parameters associated with predicting combustion noise. These parameters associated with combustion noise will be investigated in terms of their accuracy, robustness with different sensors, cycle to cycle variations in correlation to combustion noise.The parameter should be easy to implement in a real time system(low computational power) and must be evaluated on cycle to cycle basis.

## 2.1 Major Tasks

The major tasks are

- Development of a parameter for combustion noise control based on pressure traces in different speed/load points under different conditions (boost pressure, main injection timing, rail pressure, different pilot injections, pilot injection quantity, pilot injection timing, EGR rate, and coolant temperature)

- Implementation of the most promising parameters on a Rapid-Control-Prototyping system.

- Measurements on an acoustic chassis dynamometer to evaluate accuracy of the parameter.

## 2.2 Limitations

The study is performed to find out a simple parameter which can relate to combustion noise. The main aim of the parameter is to identify the relative change in combustion noise. For example, Increase in combustion noise relates to the increase in the identified parameter and decrease in combustion noise relates to the decrease in identified parameter. The parameter doesn't give any significant numeric value which can be directly related to combustion noise through numerical relations. The study also limits to the current engine under consideration, application of this study to other engines need to be studied since structure of the engine

influences the noise. The application of this study requires a cylinder pressure sensor fitted in the engine. Either a single cylinder pressure sensor or pressure sensor mounted in each engine is required. If a single cylinder pressure sensor is present, then the noise is calculated based on that single cylinder data. If each cylinder is fitted with cylinder pressure sensor, then the final value is calculated by averaging the values from individual cylinder. No tests have been carried out with any cylinder pressure models to replace the cylinder pressure sensor.

# 3 FRAME OF REFERENCE

*This chapter presents the overview of closed loop combustion control and its advantages in diesel engines and the overview of combustion noise control.*

With the increasing emission norms and ever increasing customer demands, new technologies and features are getting incorporated in modern day engines and vehicles. With these new features and technologies, the engine management systems are becoming more complex with increasing number of parameters to control. This often results in increase in the calibration effort, number of test and validation tests. With the development of low cost cylinder pressure sensor, idea of in-cylinder combustion control is viable in diesel engines.

## *3.1 Closed loop combustion control in diesel engines*

Closed loop combustion control in diesel engines has several advantages over conventional combustion control. In conventional control, parameters such Mass flow of air, rail pressure, boost pressure etc. are controlled using a closed loop or without closed loop to control emissions and fuel consumption. These have no direct feedback about the combustion process or exhaust emissions.

But in closed loop combustion control, parameters which have direct influence on combustion, emission and fuel consumption such as IMEP, start of combustion , total heat release rate, location of 50% burned mass, location of maximum pressure etc. that are calculated from the cylinder pressure, can be controlled in close loop over real time engine operation. Novel control concepts are developed, which improves the combustion efficiency resulting in lower emission and better fuel consumption also accounting for the combustion noise.

Various combustion control concepts that are possible with cylinder pressure based closed loop combustion control are

- Control of centre of combustion
- Control of IMEP
- Control of combustion noise and stability
- Control of pilot combustion
- Combustion rate/pressure gradient control
- Combustion control for regeneration or heating combustion modes
- Combustion rate shaping

- Digital combustion rate shaping
- Real time combustion control

Either individual control concept or a cascaded control concepts based on the application requirements can be implemented [8].

## *3.2 Advantages of Closed loop combustion control*

Some of the advantages of closed loop combustion control system include

- Faster and more accurate combustion control results in lower engine emissions
- Closed loop control of combustion parameters reduces the cycle to cycle variation
- Engine calibration time is reduced using cylinder pressure based engine management since calibration is based on thermodynamic models.
- Less correction maps are necessary to compensate for combustion events since this information is known from the cylinder pressure data.
- Compensation for variation in Injection quantity between different injectors
- Compensation for cylinder to cylinder variations.
- Improved cold start and altitude performance of the engine.
- Control of combustion noise
- Compensation for varying levels of fuel quality
- Compensation for aging of components.

Below figure shows some advantages of the closed loop combustion control for diesel engines. (Internal)

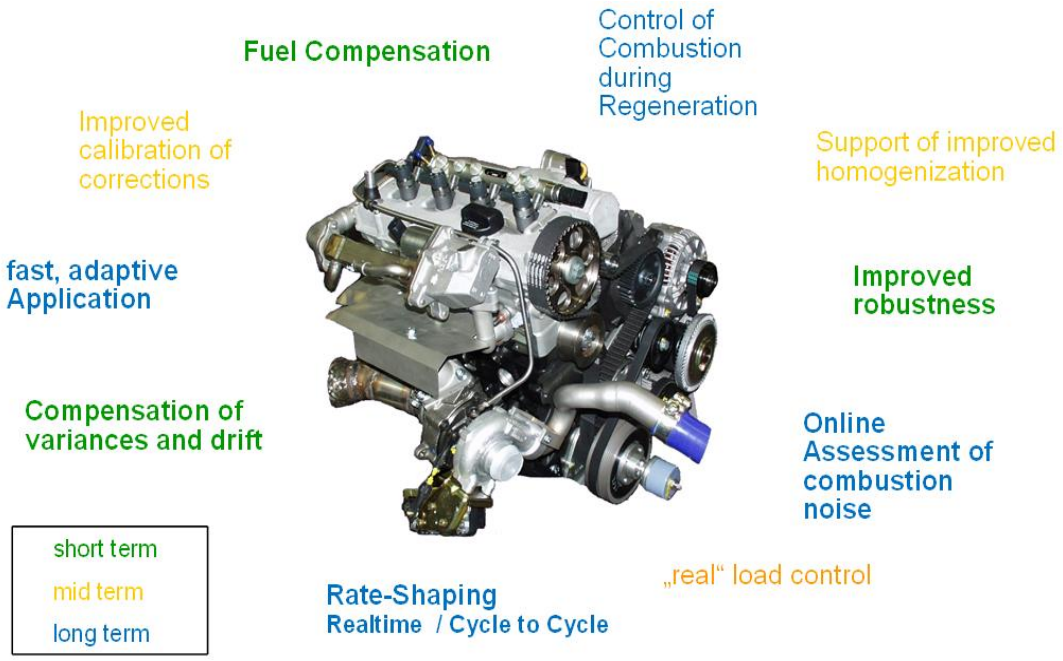


Figure 1. Advantages of closed loop Combustion Control[2]

## 3.3 Combustion noise and stability control

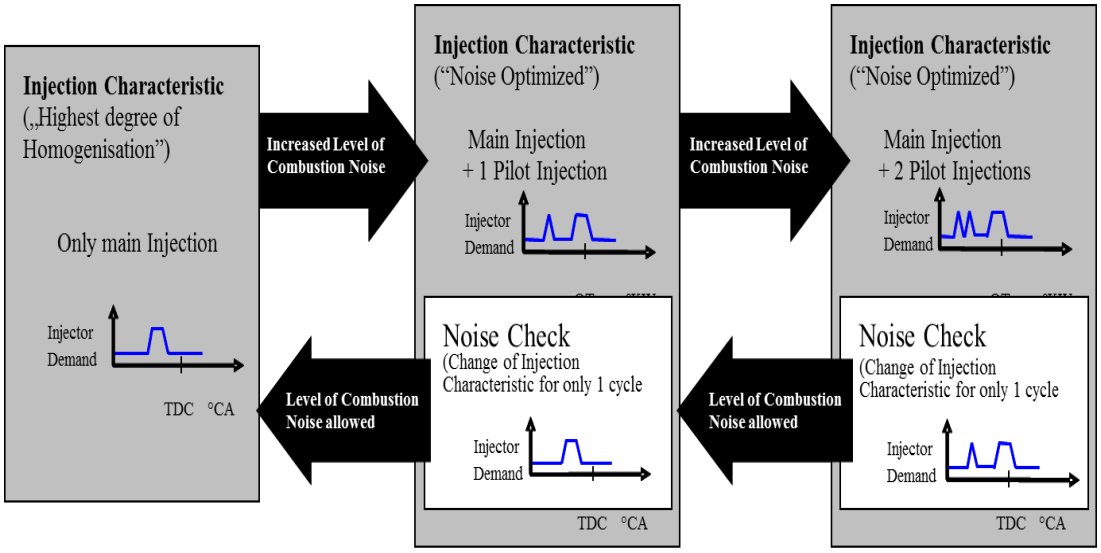


Figure 2. Combustion noise Control [3]

The above figure shows the current state of art technology used in closed loop combustion control for reducing combustion noise.

It uses number of pilot injections as a control parameter for limiting combustion noise. The control model decides on the number of pilot injections based on the combustion noise level, which is calculated from the cylinder pressure sensor. Operating without pilots results in huge benefits of smoke from the engine, but increases the noise from the engine. The controller

model decides automatically on either operating with main injection, single pilot or double pilot according to the calculated combustion noise level.

Combustion noise level which predicts the direct combustion noise can be incorporated in real time analysis and hence can be used for closed loop control. However, indirect combustion noise and flow noise associated at higher loads are not accurately predicted by the Combustion noise level. It also requires very precise injection characteristics and high performance processors. Accurate calculation of combustion noise level requires pressure data with 0.1° CA. These limitations have prompted for development of a new parameter which correlates well with combustion noise at different operating conditions and easy to implement for real time control. [5]

# 4 COMBUSTION NOISE AND PARAMETER DEFINITION

*In this chapter the basics of combustion noise and the parameters chosen for relating combustion noise is defined.*

## 4.1 Combustion noise

Noise radiated from the engine can be divided into mechanical noise, accessory noise and combustion noise. Mechanical noise is the noise radiated from the engine without combustion and it is almost independent of load and is a function of the engine speed. Combustion noise is the noise due to combustion. Combustion noise can be further subdivided into direct combustion noise and indirect combustion noise, Flow noise, which results due to the surface radiation of the airflow through components, excited by the air mass flow and radiated by the intake and exhaust system which is mainly dependent on the load can also be considered as combustion related noise, since flow requirements vary directly based on the boundary conditions of the combustion.

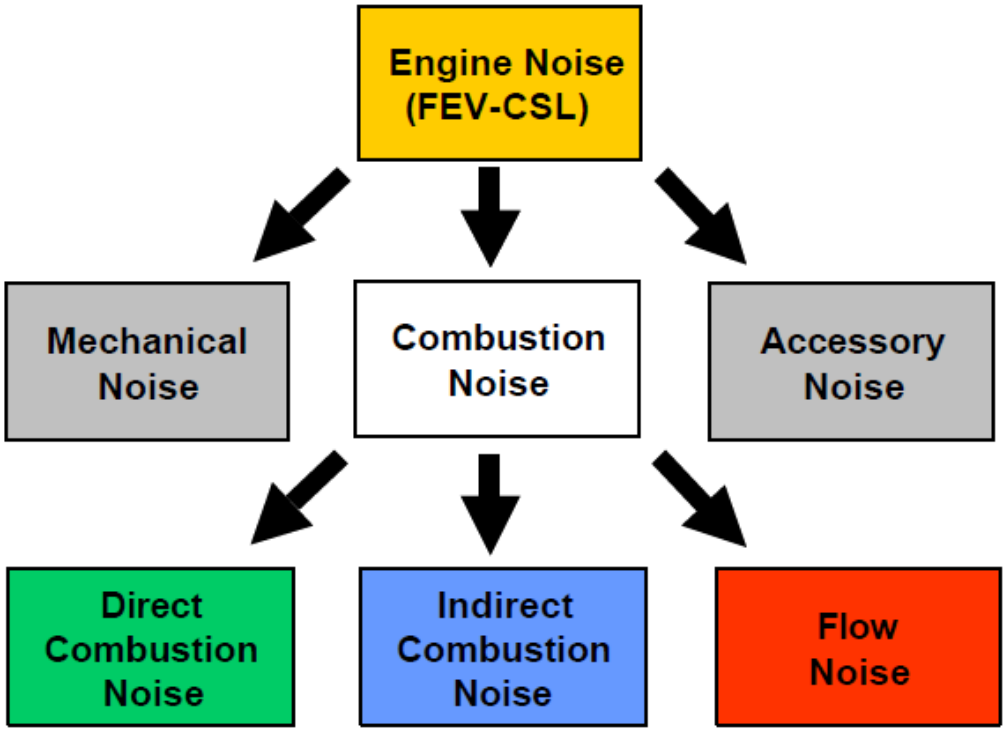


Figure 3. Engine noise shares [4]

The above figure shows the various noise shares associated with engine noise.

Diesel combustion noise is primarily due to the self-ignition of the mixture resulting in rapid pressure rise inside the cylinder. This steep increase in pressure results in oscillation of the gas inside the cylinder. Direct combustion noise is caused by the effects of combustion pressure on the surrounding engine structure while assuming that no clearances occur. It is transmitted through an external and internal transmission path. External transmission path is considered as the direct effect of combustion chamber pressure on the cylinder wall, while transmission through piston, connecting rod and crankshaft to the structure is considered as the internal transmission path. The internal transmission path is generally dominant.

Indirect combustion noise contains the total excitation by rotary and piston normal force, which have a different course versus time compared to the gas force. It contains e.g. piston slap noise, crankshaft torsion and cyclic speed fluctuations caused noise, such as gear rattle noise, in example.

Direct combustion noise relates to the cylinder pressure curve over the crank angle. It also relates to the total excitation (force and impact) due to the gas force and all other forces inside the engine that have a similar course versus time. A certain correlation to the cylinder pressure gradients exists. Indirect combustion noise follows the torsion force and contains the total excitation by rotary and piston normal forces that have a different course versus time compared with the gas force, a certain correlation to “peak pressure x leaver arm” exists.

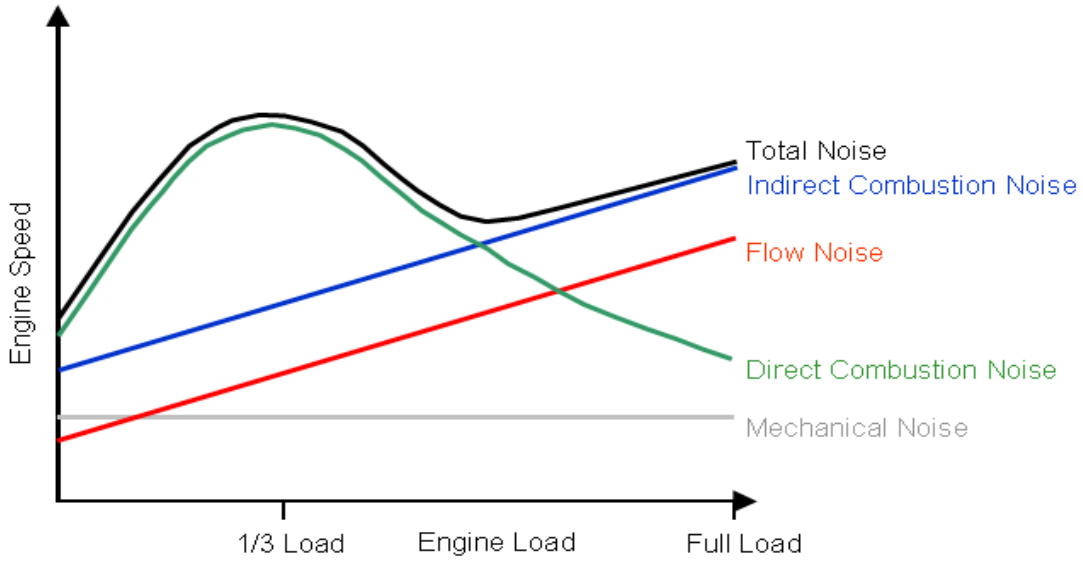


Figure 4. Contribution of different noise shares [5]

The above figure shows the various noise shares from a direct injection diesel engine as a function of engine load.

A diesel part load noise increase typically is caused by direct combustion noise. But at higher loads, share of direct combustion noise decreases due to increase in the pressure and temperature inside the cylinder which results in shorter ignition delay and then less cylinder pressure gradient. Indirect combustion noise and flow noise linearly increases with load, caused by increase of peak pressures and air mass flow. Mechanical noise is constant as it is dependent on engine speed.

## 4.2 Definition of parameters for combustion noise analysis

The following article contains the brief definition of parameters that were investigated for predicting combustion noise.

### 4.2.1 Combustion Sound Level – CSL

CSL predicts engine noise level based on estimating the direct combustion noise, indirect combustion noise, flow noise and mechanical noise using engine specific weighting functions. Different shares of engine noise can be calculated and analysed. CSL shows very good correlation to measured microphone noise measurement. With standard weighting function, there are some minor differences with the absolute values.

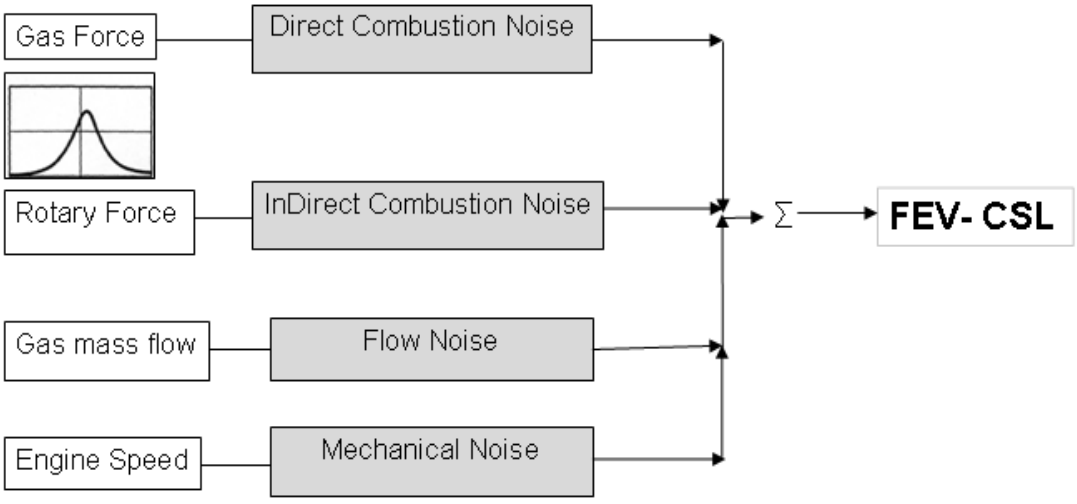


Figure 5. Combustion sound level [4]

CSL requires pressure data of 1° CA resolution, but computations are complex making it ineffective to implement it in real time applications. In the current project, the other noise

related parameters will be compared with CSL. During calculation of CSL, standard weighting functions were used instead of engine specific weighting functions.

### *4.2.2 Combustion Noise Level – CNL*

CNL is a single value number which corresponds to direct combustion noise. CNL serves as a relative judgement to combustion and combustion variants in respect to noise excitation. It is calculated by performing a fast Fourier transform on the pressure signal and then weighting the signal with a standard attenuation functions.

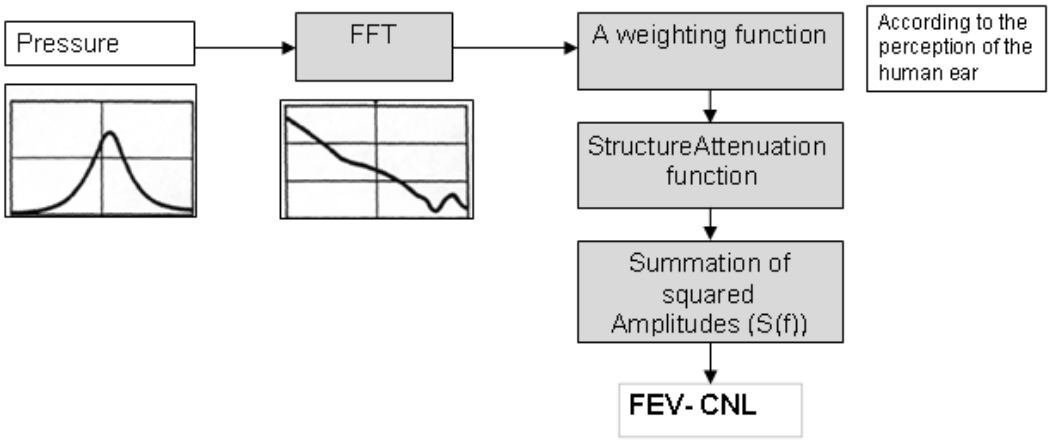


Figure 6. Combustion noise level [6]

### *4.2.3 Pressure parameters*

Pressure parameters such as maximum pressure ($P_{max}$), crank angle at which the maximum pressure occurs ($\alpha_{Pmax}$), rate of pressure rise due to combustion with respect to crank angle and time($dP/d\alpha_{max}$, $dP/dt_{max}$), angle at which the max rate of pressure rise occurs($\alpha_{dP/dtmax}$). Since pressure variation inside the cylinder is a major source of noise all the pressure related parameters is of relative importance for assessing combustion noise.

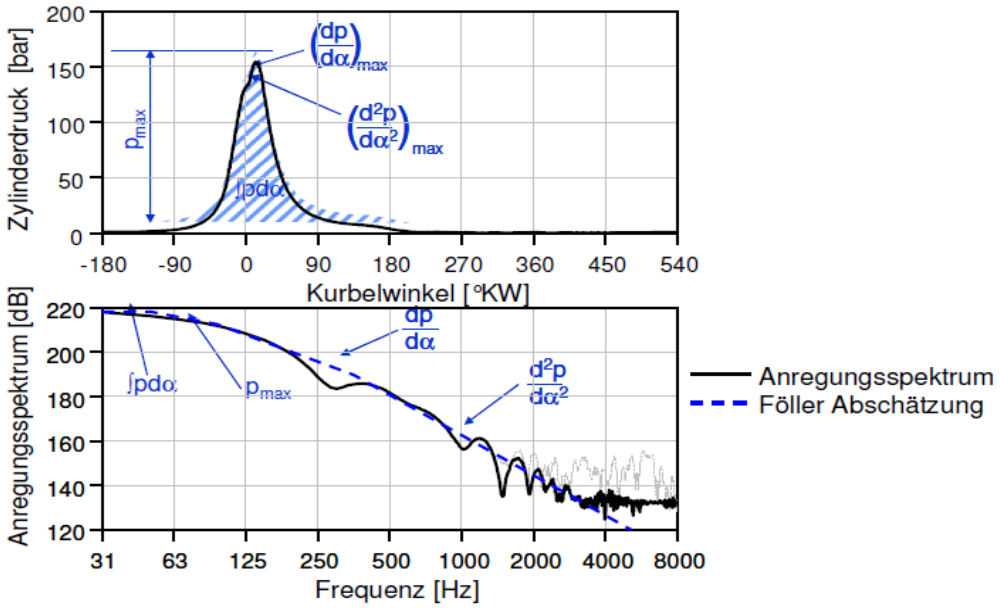


Figure 7. Cylinder pressure in time domain and frequency domain [7]

Rate of pressure rise due to combustion excites the gas inside the cylinder. These oscillating gases inside the cylinder result in vibration of the block, one of the major sources of emitted noise. The dependence of maximum pressure gradient on engine speed can be decoupled by changing the rate of pressure rise over crank angle to rate of pressure rise over time.

### *4.2.4 Heat release parameters*

Heat release rate which is an indicator for the combustion happening inside the cylinder. Maximum value of heat release rate due to combustion with respect to crank angle and time ($dQ/d\alpha_{max}$, $dQ/dt_{max}$), angle at which the max rate of pressure rise occurs ($\alpha_{dQ/dtmax}$).

Heat release value is dependent of the calorific value of the fuel. Characteristic combustion noise varies according to the fuel used. Heat release rate is strongly coupled with the pressure rise inside the cylinder due to combustion. Rate of heat energy release over crank angle is calculated from the model Cumulative heat release can be determined by summing the individual values and then mass fraction burned can be calculated from the normalized cumulative values.

Although the pressure parameters are more representive of combustion noise, at some engine operating condition especially when the combustion starts after TDC, effect of pressure related parameters are offset by the increasing volume during the expansion stroke. Heat release parameter which is strongly coupled with the pressure rise is not much influenced by this increase in volume during the expansion stroke.

### 4.2.5 Combined parameter 1

Parameter combining maximum pressure gradient with respect to time and then ignition delay ($(dP/dt_{max})/ti$).

Maximum rate of pressure rise depends on the premixed combustion, which depends on the ignition, so the rate of pressure rise over time normalised with ignition delay can corresponds to some components of the combustion noise.

### 4.2.6 Combined parameter 2

Parameter combining maximum pressure gradient with respect to time, maximum pressure and then ignition delay ($(dP/dt_{max})^{2}(P_{max})^{0.5}/t_i^{2}$).

Maximum rate of pressure rise raised to the power of two multiplied by maximum value of pressure raised to the power of half divided by the square of ignition delay.

All the above mentioned parameters are included in the Simulink model along with some basic combustion parameters such as mass fraction burned (10 %, 50 %, 90 % MFB), 10 % mass fraction burned refers to the crank angle at which the 10 % of the combustion mixture burns, Indicated mean effective pressure (IMEP) refers to the work done inside the volume over the four cycles divided by swept volume, Pumping mean effective pressure (PMEP) refers to the work done by the piston on the gases during suction and exhaust stroke divided by swept volume, net indicated mean effective pressure(net IMEP) refers to the work done during the compression and expansion stroke divided by swept volume. These parameters serve as an indicator for the combustion happening inside the cylinder.

# 5 METHODOLOGY

*In this chapter the methodology used for analyzing the cylinder pressure sensor to derive a parameter for combustion noise control and then validation test setup is described.*

## 5.1 Combustion noise

The study involves analysis of cylinder pressure traces taken from engine test bed at various engines operating condition to predict a suitable parameter for combustion noise. The various parameters associated with combustion noise are calculated from the cylinder pressure traces using Simulink model and are then plotted against the reference combustion noise parameter (Combustion Sound Level). Combustion sound level is calculated from the cylinder pressure traces using Foeller estimation principle.

An existing 0-dimensional single zone model of the combustion chamber is incorporated with the required combustion noise parameters. Cycle averaged (50 cycles) cylinder pressure traces and cycle resolved (50 cycle) pressure traces with a resolution of 0.1° crank angle, measured with two different pressure sensors at various engine operating conditions are processed using the model to obtain the necessary parameters related to combustion noise. Then the calculated parameters are correlated with the combustion sound level. The most promising parameters predicting combustion noise are implemented in the Rapid Control Prototyping (RCP) system and then verified with measurements on an acoustic chassis dynamometer.

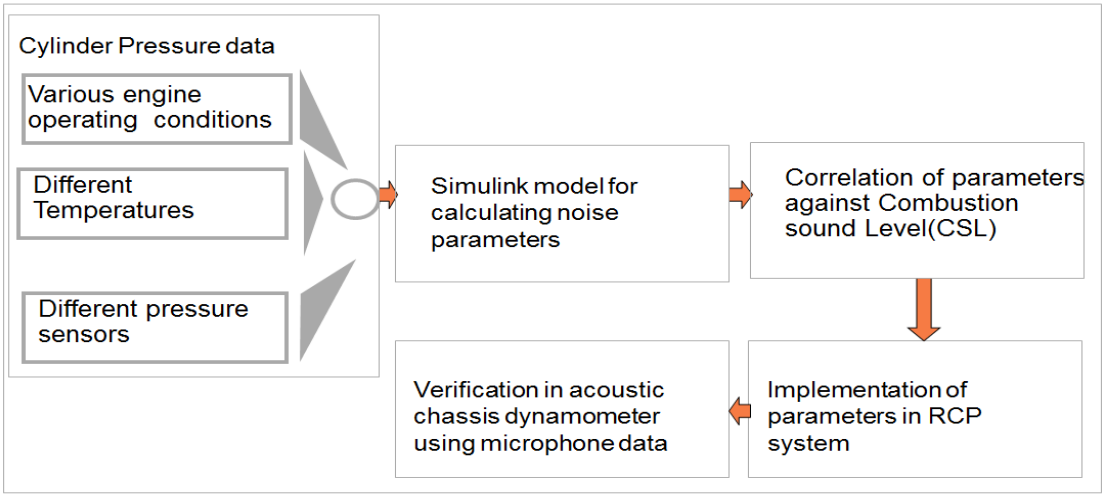


Figure 8. Methodology

## 5.2 Microphone location

For acoustic chassis dynamometer measurement, the vehicle was fitted on a roller inside an anechoic chamber. Noise measurements were recorded from four microphones mounted at different locations.

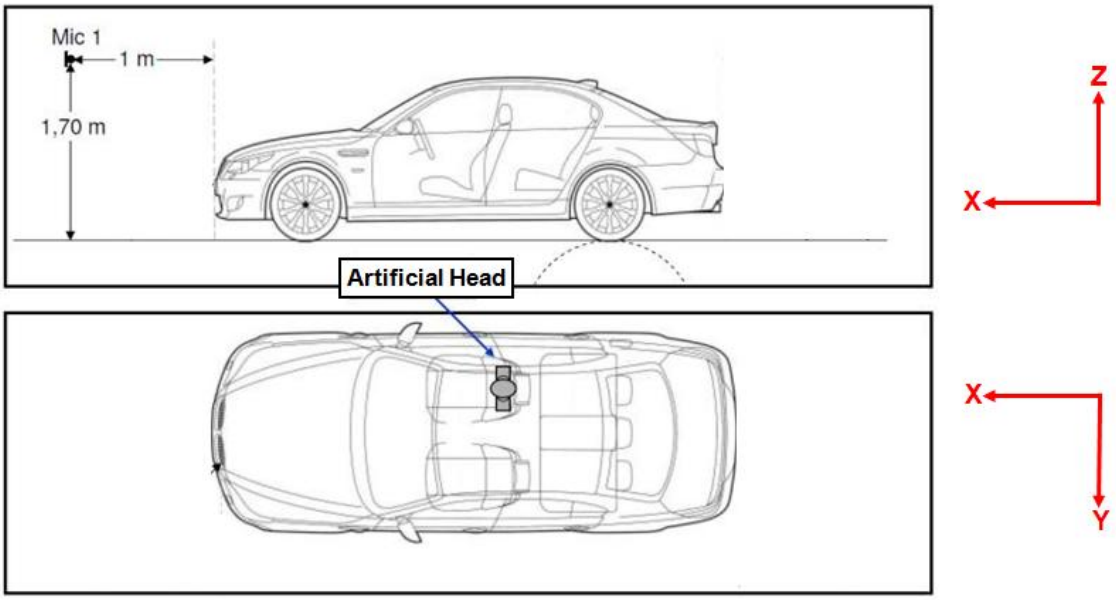


Figure 9. Microphones location

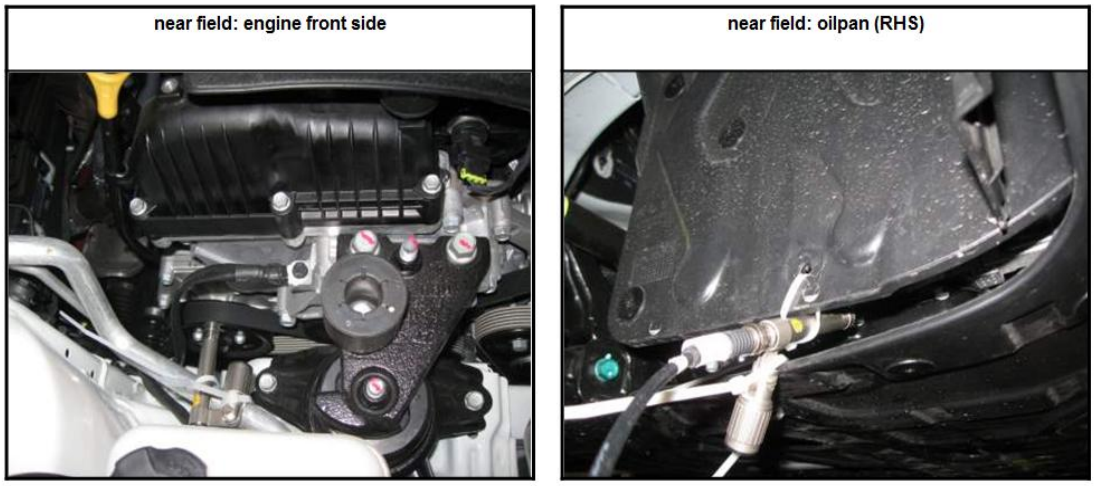


Figure 10. Microphones location inside the engine compartment

The microphone location was based on the noise level assessment inside the passenger compartment (Acoustic head) and pass by noise assessment (Microphone located in front of

the vehicle). To access the combustion noise, two microphones were placed inside the engine compartment. One located beneath the oilpan and the other on the front side of the engine as shown in figure 4.7.

The microphones must be located nearby plain engine surface, where the surface radiates the noise. Care should be taken that the microphones should be placed away from the intake or exhaust system and away from the driving belt.

# 6 RESULTS

*In this chapter the results that are obtained from the initial cylinder pressure sensor analysis and then the validation test results are presented.*

## 6.1 Test bed data analysis results

### 6.1.1 Cycle averaged pressure data (50cycles)

#### Correlation to CSL

Noise parameters calculated from the pressure traces using the model are plotted against the reference CSL. Plotted data includes steady state operating condition, in which various sweep variables such as EGR demand, rail pressure, pilot 1 & pilot 2 quantity and timing, boost pressure and main timing are varied at three different coolant temperatures 90° C, 60° C and 30° C and at various speed and load conditions.

The following figure shows the correlation of noise parameters to CSL. The correlation value in the legend section refers to the linear correlation coefficient between CSL and the respective parameter.

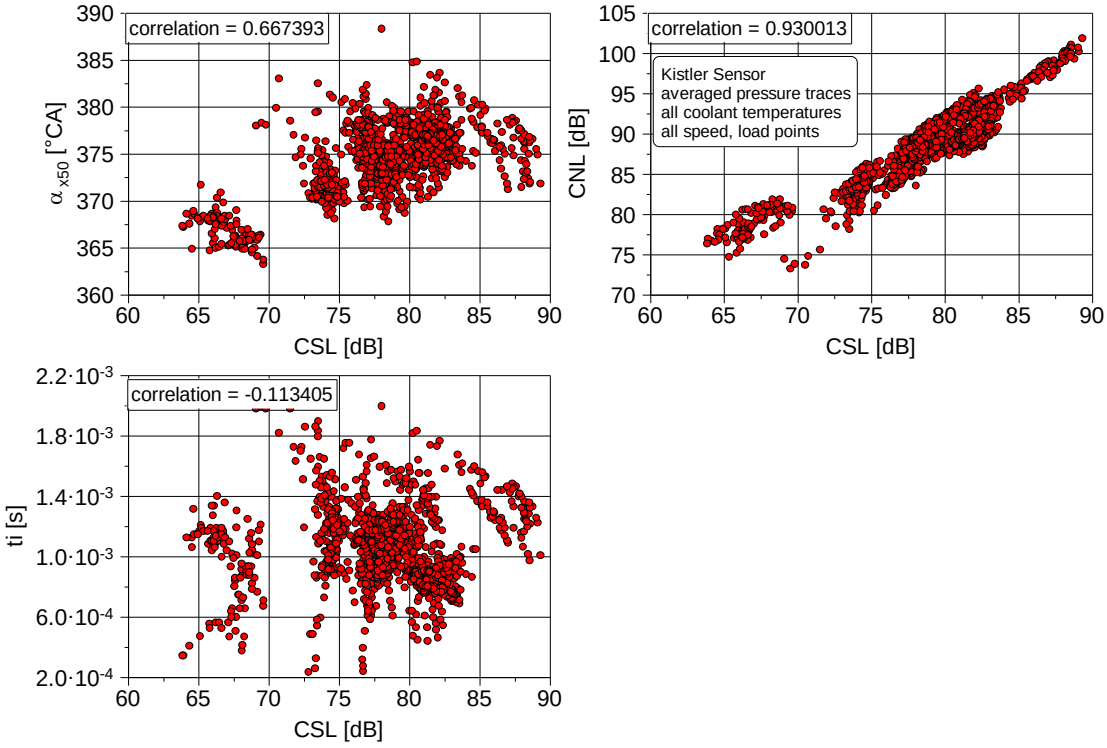


Figure 11. Noise parameters correlation to CSL

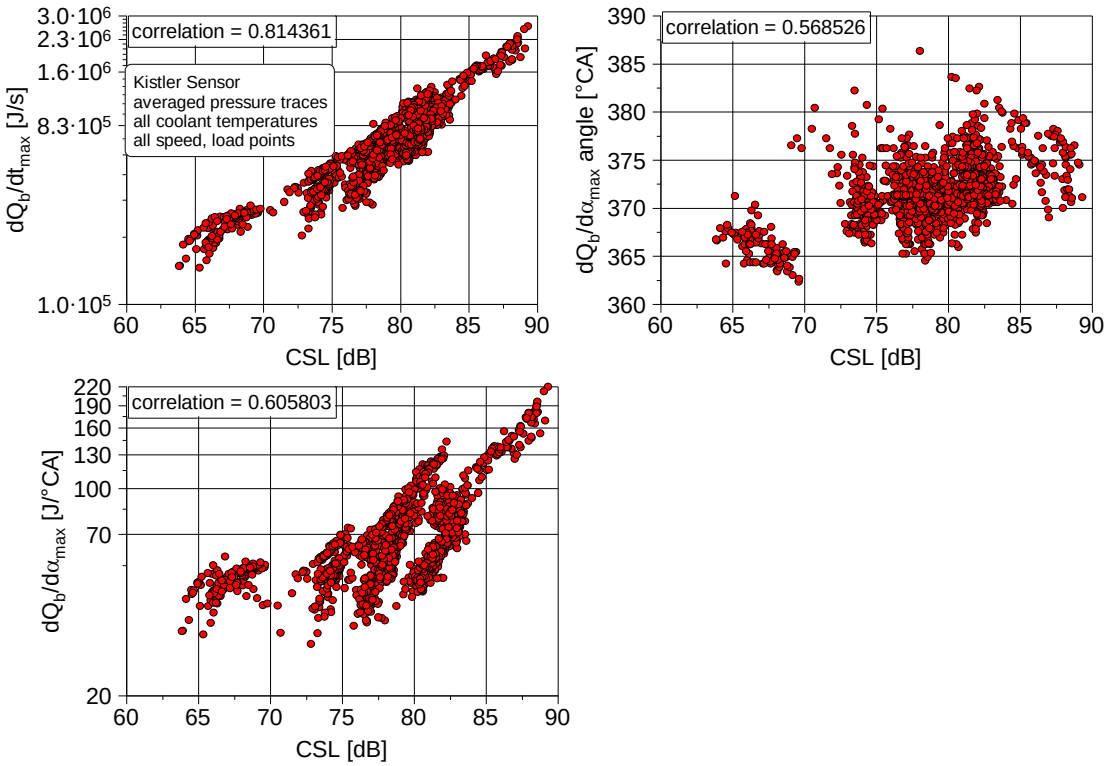


Figure 12. Heat release parameters correlation to CSL

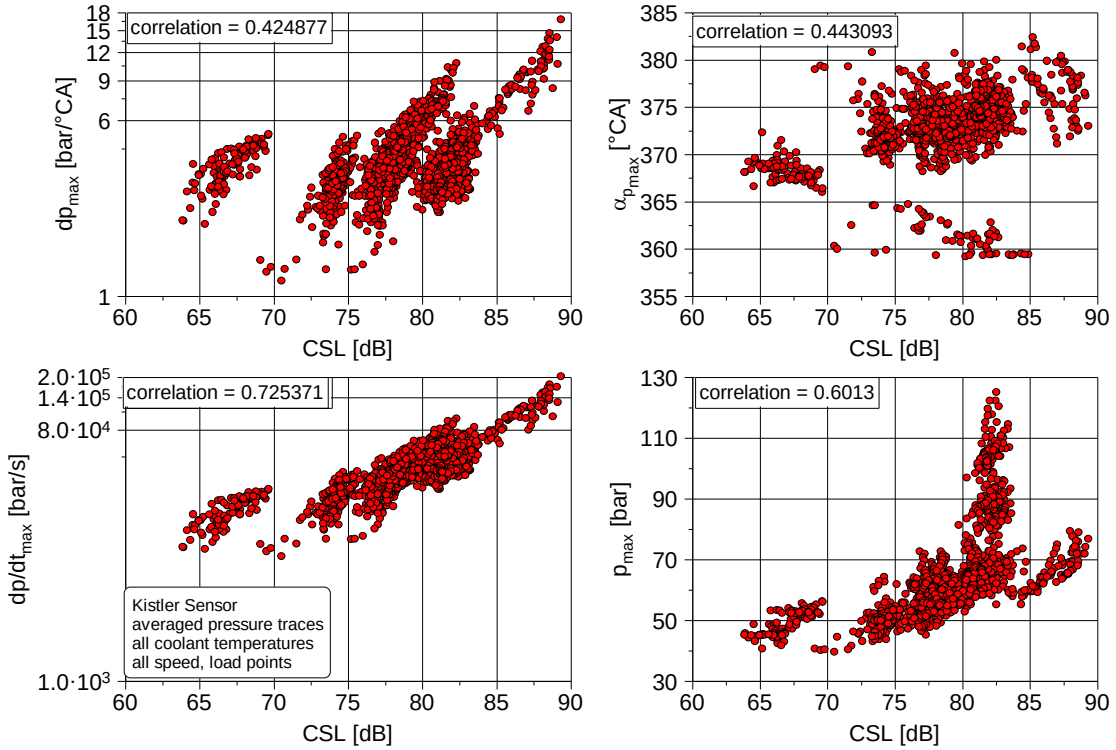


Figure 13. Pressure parameters correlation to CSL

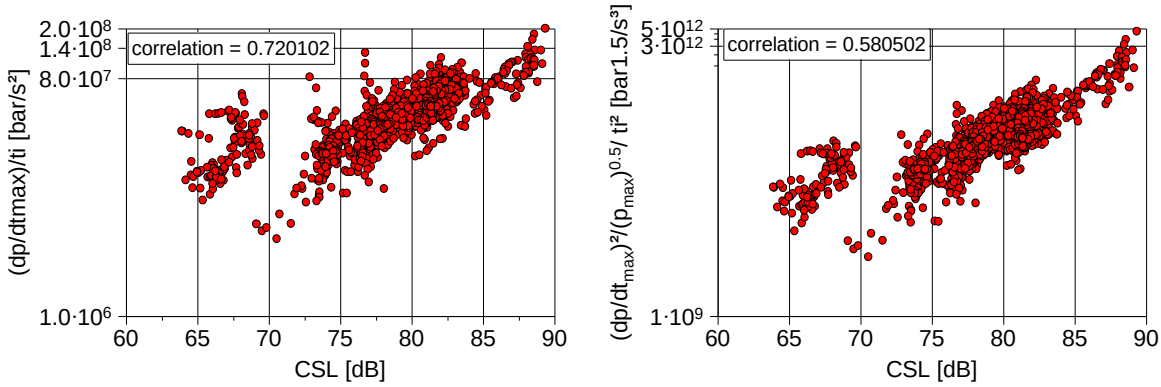


Figure 14. Combined parameters correlation to CSL

Table 1. Linear correlation coefficient value of noise parameters against CSL.

| Parameters | Kistler | Beru | Kistler vs. Beru |
|---|---|---|---|
| **CNL [dB]** | 0.93 | 0.92 | 0.91 |
| **$t_i$ [s]** | -0.11 | 0.07 | 0.78 |
| **$dQ_b/d\alpha_{max}$ [J/°CA]** | 0.61 | 0.59 | 0.92 |
| **$dQ_b/dt_{max}$ [J/s]** | **0.81** | **0.81** | **0.96** |
| **$dQ_b/d\alpha_{max\_angle}$ [°CA]** | 0.57 | 0.50 | 0.53 |
| **$P_{max}$ [bar]** | 0.60 | 0.63 | 0.99 |
| **$\alpha_{Pmax}$ [°CA]** | 0.44 | 0.46 | 0.55 |
| **$\alpha_{dPmax}$ [°CA]** | -0.14 | -0.07 | 0.87 |
| **$dp_{max}$ [bar/°CA]** | 0.43 | 0.34 | 0.95 |
| **$dp/dt_{max}$ [bar/s]** | 0.73 | 0.70 | 0.96 |
| **$(dp/dt_{max})/t_i$ [bar/s²]** | 0.72 | 0.72 | 0.92 |
| **$\alpha_{x50}$ [°CA]** | 0.67 | 0.14 | 0.97 |
| **$(dp/dt_{max})^2/(P_{max})^{1.5}/t_i^2$ [$bar^{1.5}/s^2$]** | 0.58 | 0.57 | 0.95 |

The table contains the linear correlation co-efficient value of noise parameters against CSL measured with Kistler and Beru pressure sensor. The fourth column Kistler vs. Beru shows the linear correlation between the values predicted with Kistler and Beru sensor.

CNL shows good correlation to CSL. All the other parameters show very good correlation at only some operating points, overall correlation to CSL at all operating conditions was not significant.

### *6.1.2 Cycle resolved pressure data (50cycles)*

#### *Coefficient of variation analysis*

For cycle resolved pressure data with 50 consecutive cycle's data, cycle to cycle variation of all the parameters can be studied by calculating the coefficient of variation, which is the standard deviation of the 50 cycles divided by the mean value of the 50 cycles.

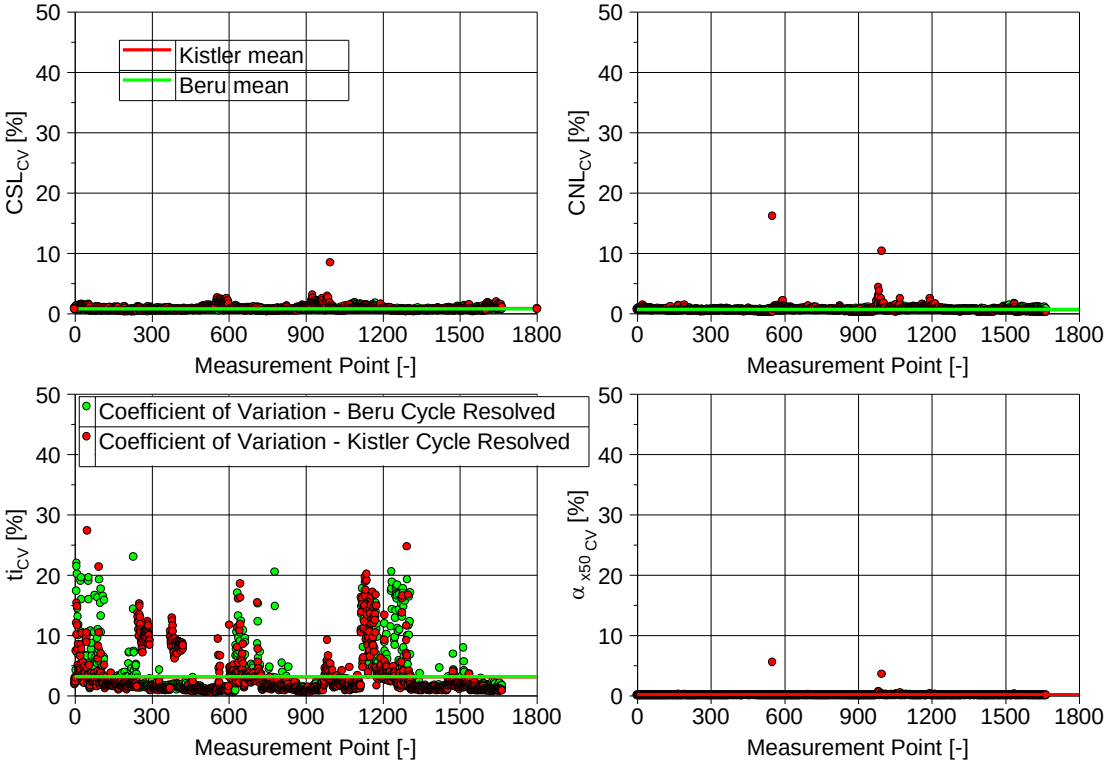


Figure 15. Coefficient of variation for the 50 cycles – Noise parameters

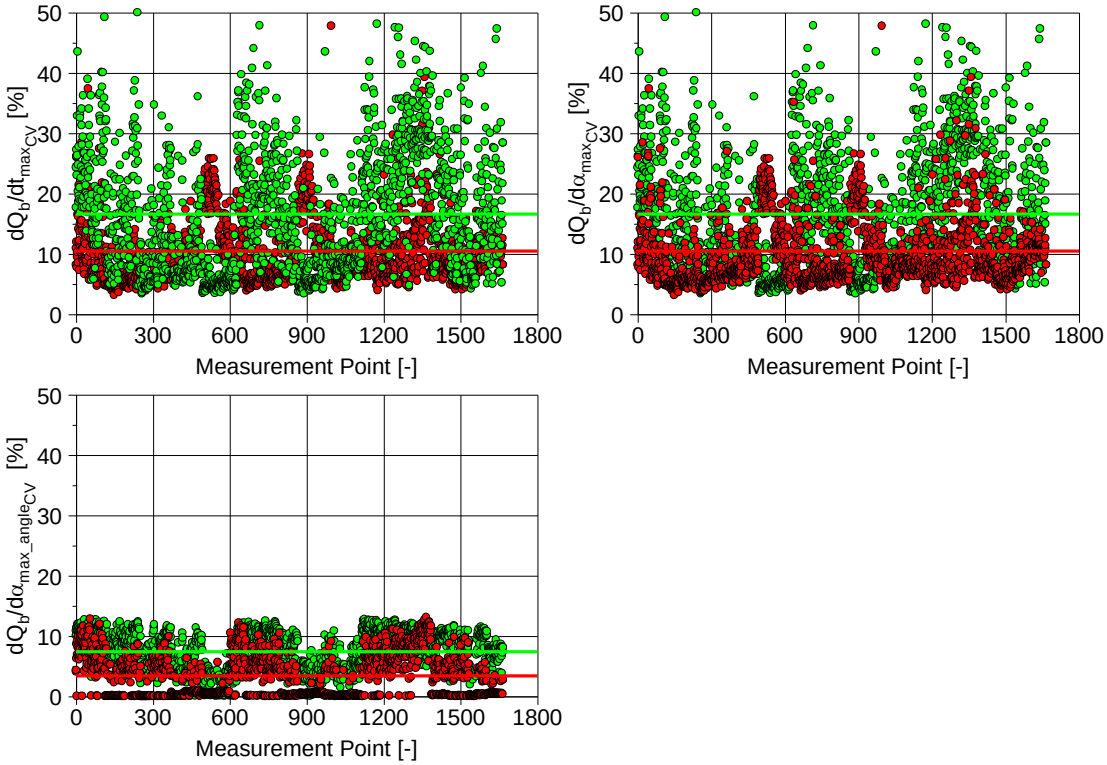


Figure 16. Coefficient of variation for the 50 cycles – Heat release parameters

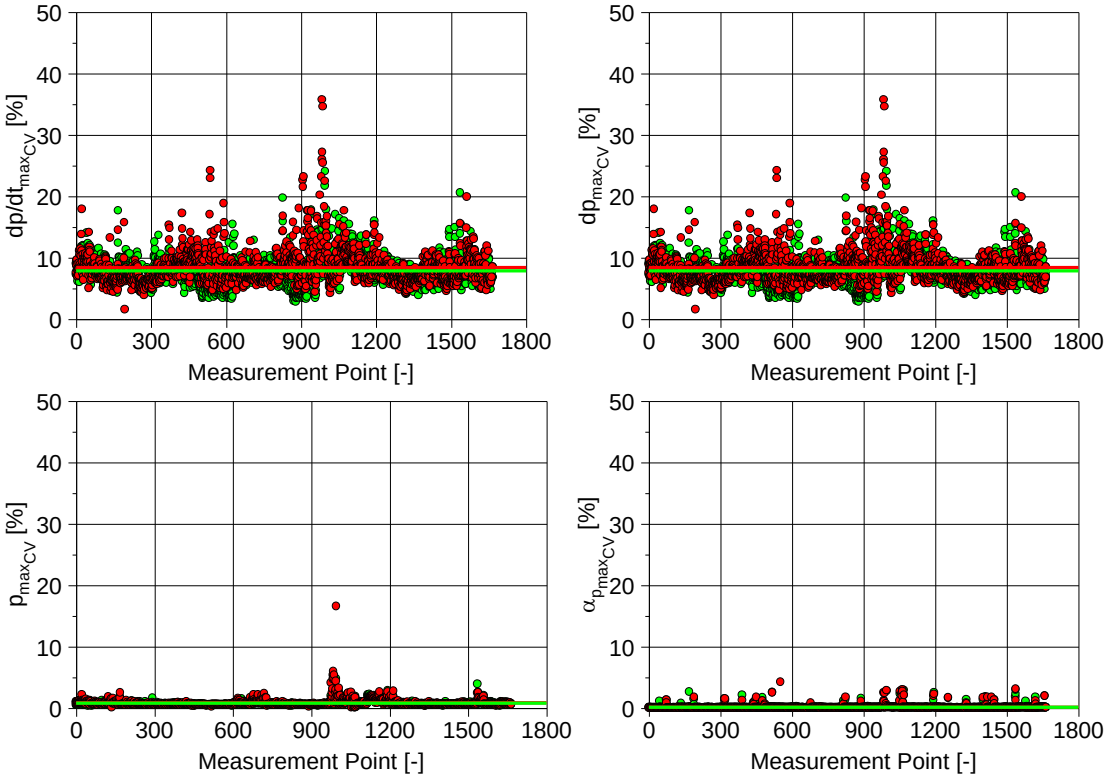


Figure 17. Coefficient of variation for the 50 cycles – Pressure parameters

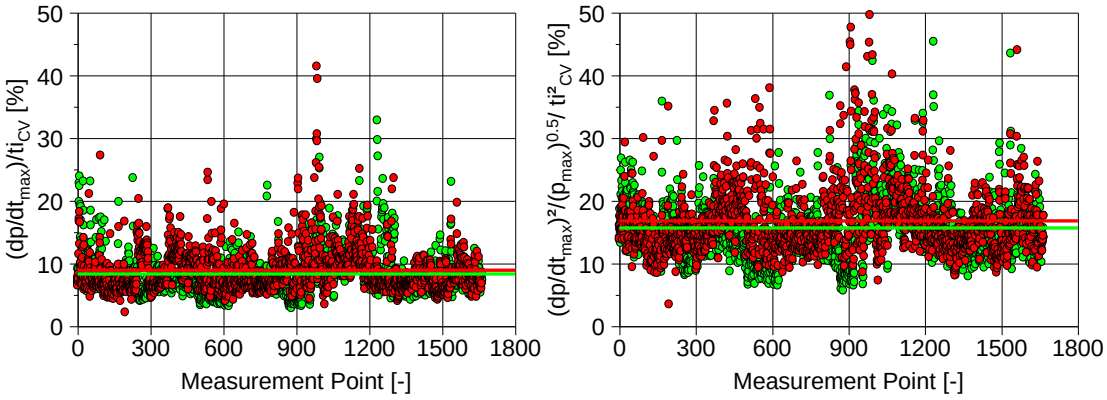


Figure 18. Coefficient of variation for the 50 cycles – Combined parameters

The above figure shows the coefficient of variation for all the calculated parameters containing all measurement points.

Coefficient of variation for CSL and CNL are very less indicating very high signal strength. Co-efficient of variation for $dQ/dt_{max}$ for most of the load points with Kistler sensor data was less (around 10). At very high load points, 2000 rpm 14 bar BMEP and 2200 rpm 9 bar BMEP coefficient of variation was higher. On analysing the pressure traces for these load points, high amplitude noise in the pressure data around Top Dead Centre (TDC). The below

figure shows the calculated heat release value at 2000 rpm 14 bar BMEP normal operating condition, 360° crank angle refers to the TDC.

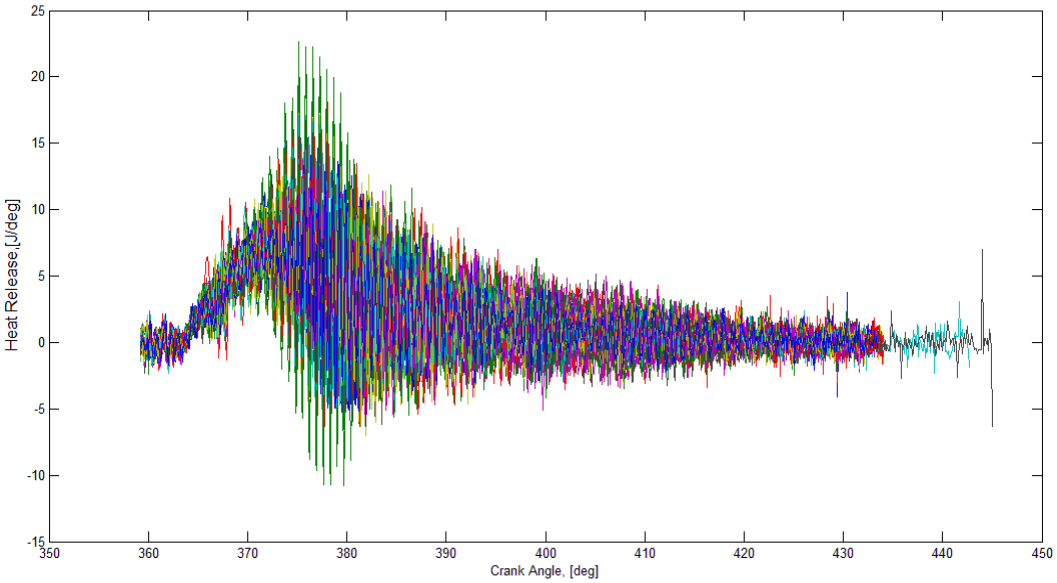


Figure 19. Maximum rate of heat release at 2000 rpm 14 bar BMEP Kistler sensor

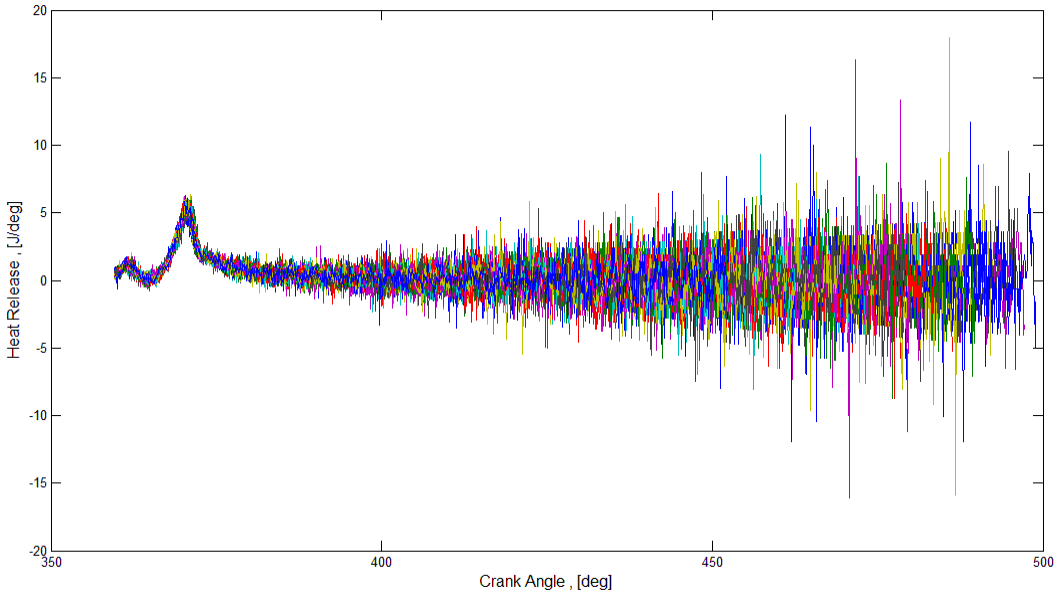


Figure 20. Maximum rate of heat release at 1250 rpm 3 bar BMEP Beru sensor

Co-efficient of variation for $dQ/dt_{max}$ with Beru sensor was higher at low and medium loads and was less at high load points. This was due to the noise in the pressure signal. A frequency filter incorporated for the pressure signal in the model would eliminate the problem. But for real time implementation, frequency filter will introduce some delay and requires

considerably higher computational power. Since the noise in the signal gets amplified with increase in volume, the model was modified to calculate max rate of heat release within 60° after TDC. After the changes in model, the concerned high load points for Kistler sensor and low load points for Beru sensor was simulated again and lower co-efficient of variation values was observed.

## 6.2 Evaluation

Based on the above discussions and criteria an evaluation was made for all the parameters to decide which parameter can be a good compromise in predicting combustion noise and requires less computational power and ease of implementation

Table 2. Rating of noise parameters for various criteria

| Parameters | Accuracy | Robustness | | Signal to Noise ratio | | Calculation Demand | Resolution Requirement | Overall |
|---|---|---|---|---|---|---|---|---|
| | | CA | CR | Kistler | Beru | | | |
| **CSL[dB]** | | ++ | ++ | ++ | ++ | - | ++ | ++ |
| **CNL[dB]** | ++ | + | + | ++ | ++ | - | 0 | ++ |
| **$dQ_b/dt_{max}$[J/s]** | ++ | + | 0 | + | + | + | + | + |
| **$P_{max}$[bar]** | + | ++ | + | ++ | ++ | ++ | ++ | + |
| **$\alpha_{Pmax}$[°CA]** | 0 | -- | 0 | + | ++ | ++ | ++ | 0 |
| **$dp/dt_{max}$[bar/s]** | + | + | ++ | 0 | 0 | + | - | + |
| **$(dp/dt_{max})/t_i$ [bar/s²]** | + | - | 0 | 0 | 0 | + | 0 | 0 |
| **$\alpha_{x50}$** | + | ++ | + | ++ | ++ | ++ | ++ | ++ |
| **$(dp/dt_{max})^2/(P_{max})^{1.5}/t_i^2$[$bar^{1.5}/s^2$]** | 0 | + | + | -- | -- | + | 0 | - |

- Accuracy – Based on parameter linear correlation coefficient values with CSL
- Robustness – Based on variation with two different sensors (Kistler and Beru).
  - CA - Cycle averaged data
  - CR - Cycle resolved data
- Signal to Noise ratio – Based on the coefficient of variation values calculated for the 50cycle
- Calculation Demand – Based on computational power and time required.
- Resolution requirement – Based on resolution of pressure sensor required for accurate prediction.
- Overall – overall estimation of the above mentioned criteria.

Table 3. Rating of noise parameters for various criteria

| **Value** | **Rating** |
|---|---|
| ++ | Very strong |
| + | Strong |
| 0 | Fair |
| - | Weak |
| -- | Very weak |

CSL shows high robustness with respect to different sensors. CNL correlates well with CSL and shows high robustness with respect to different sensors as well as a high signal-to-noise ratio but implementing CNL in real time requires more computational power and higher resolution pressure signal. The next parameter which has a good correlation to CSL and a good compromise on calculation demand, resolution demand and overall requirements was $dQ/dt_{max.}$ It shows high robustness with respect to different sensors. Low signal to noise ratio can be improved by incorporating some changes in the model. $dP/dt_{max}$ correlates with CSL at some conditions, shows high robustness with respect to different sensors but signal to noise

ratio is very low. $(dp/dt_{max})/t_i$ correlates with CSL at some conditions but it varies a lot with different sensors. $\alpha_{x50}$ shows high robustness and very high signal to noise ratio but accuracy is not as good as $dQ/dt_{max}$. Due to its ease of calculation and implementation over CNL, $dQ/dt_{max}$ was investigated.

### *6.2.1 $dQ/dt_{max}$ correlation to CSL at different speed and load points*

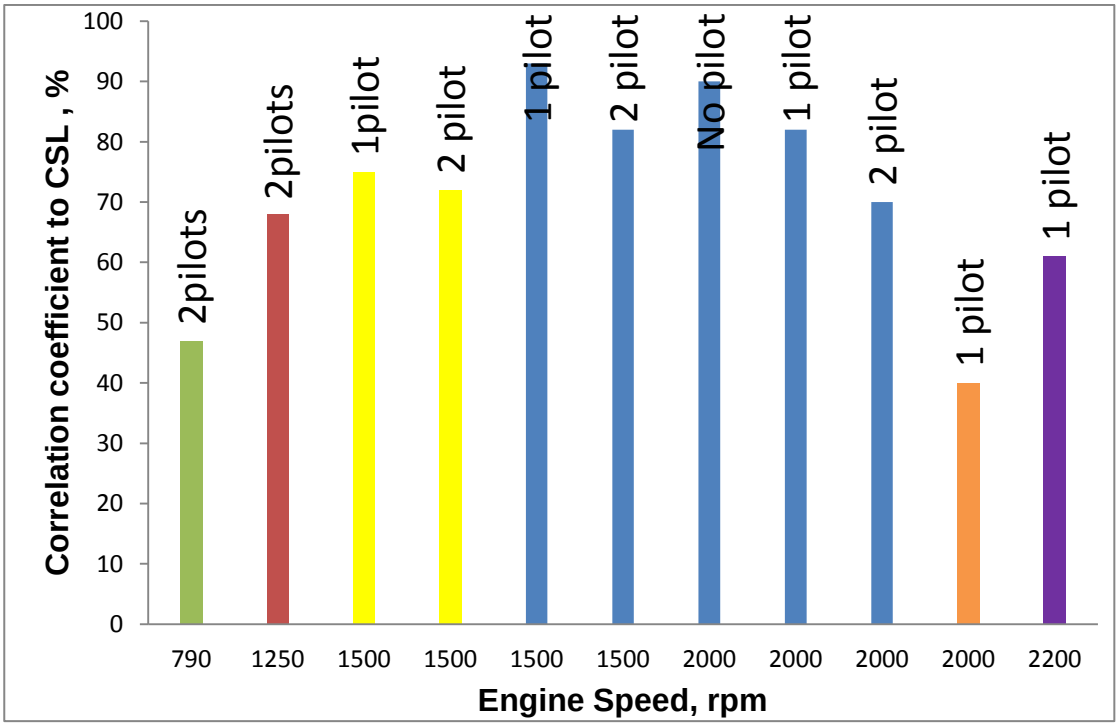


Figure 21. Maximum rate of heat release correlation to CSL at various engine operating conditions

The above figure shows the percentage of correlation between $dQ/dt_{max}$ and CSL at different speed and load points. Green color represents idle. Red color represents 3 bar Bmep load point at 1250 rpm. Yellow (4 bar Bmep) and Blue (6 bar Bmep) represents medium load points. Orange (14bar Bmep) and Violet color (9 bar Bmep) represents high load operating point. Each load point includes the various sweep points. The data shown above are measured with Kistler pressure sensor and at 90° coolant temperature. The value of the linear correlation coefficient is very less at low loads and at very high loads. In the part load range, correlation between CSL and $dQ/dt_{max}$ was higher than 70%. Also with the single pilot injection, the correlation value was higher compared to the condition with no pilot injection or two pilot injections.

### 6.2.2 Variation of $dQ/dt_{max}$ with sweep parameters

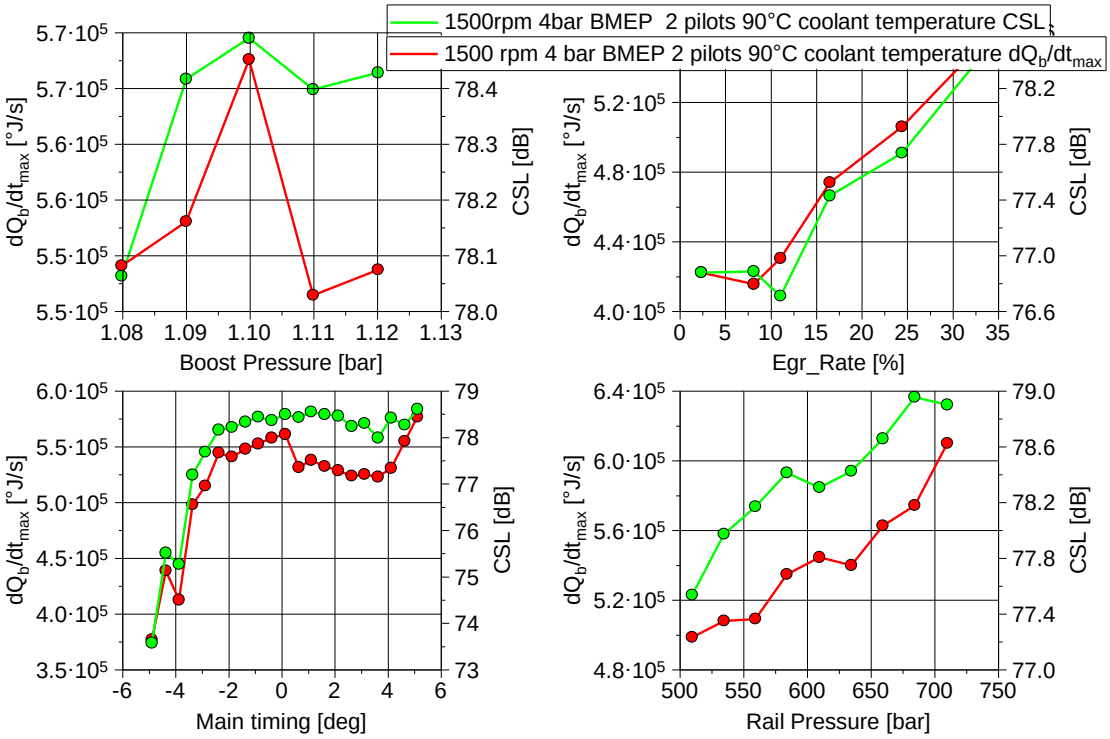


Figure 22. Maximum rate of heat release and CSL variation during parameters sweep

In the above figure, in the main timing sweep, 0° refers to the Top dead centre (TDC). Negative values refer to the respective crank angle degrees before the TDC and the positive values refer to the crank angle degrees after TDC.

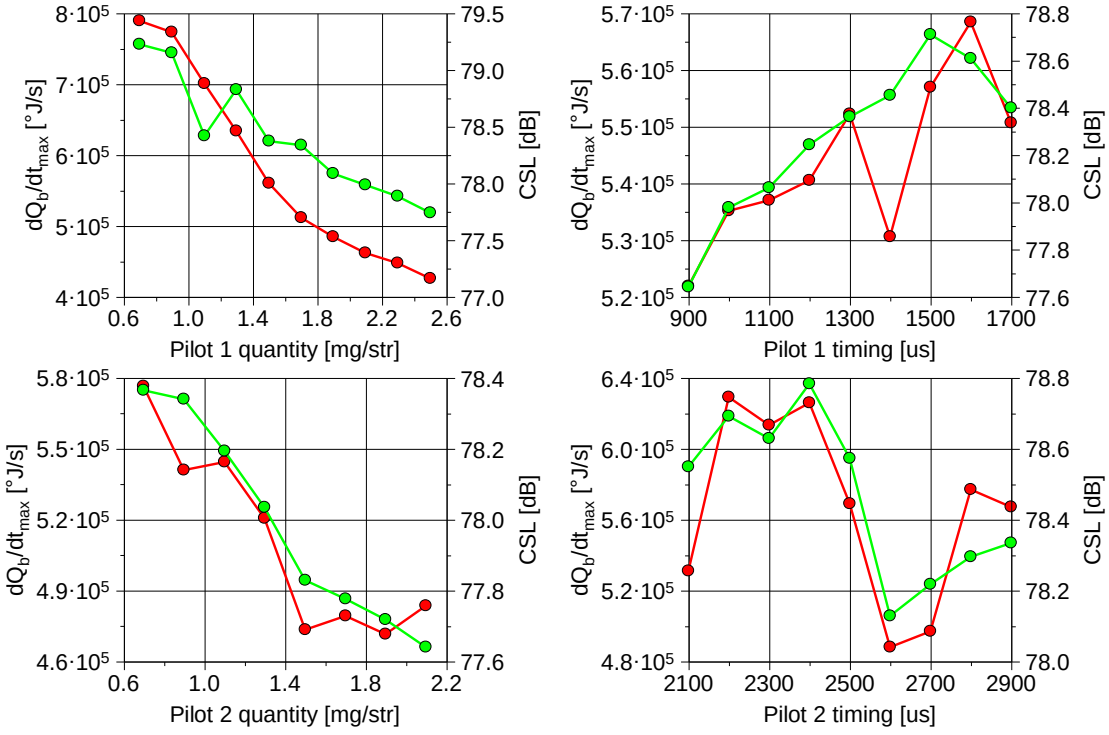


Figure 23. Maximum rate of heat release and CSL variation during parameter sweep

In the above figure, Pilot 1 timing refers to the time in microseconds before the scheduled main injection timing. Pilot 2 timing refers to the time in microseconds before the Pilot 1 timing.

The above figures shows the variation of $dQ/dt_{max}$ and CSL against various sweeps such as boost pressure, EGR rate, main timing, rail pressure, pilot 1 timing and quantity, pilot 2 timing and quantity sweep. The above data corresponds to 1500 rpm, 4 bar BMEP point with two pilot injections measured with Kistler pressure sensor. Though the relative level of increase in noise and $dQ/dt_{max}$ differs, there is a clear trend between the noise and max rate of heat release during various parameter sweeps.

Increasing the boost pressure at constant load increases the temperature for the same mass flow. This increase in air temperature with increase in boost pressure at constant fuelling decreases the ignition delay of the cycle resulting in decrease in max rate of heat release and noise after an initial rise.

Increasing the EGR rate, increase the burned gas proportion inside the cylinder which dilutes the fresh air mixture resulting in increase of the evaporation and mixing time. This results in an increased ignition delay. Even though the peak flame temperature reduces, increase in ignition delay results in more premixed fuel at the time of combustion resulting in higher $dQ/dt_{max}$, correspondingly noise also increases with increasing EGR rate.

Ignition delay is directly related to the timing of the main injection with a constant compression ratio and pilot injections. Advancing the injection well before TDC results in lower in cylinder pressure and temperature at the time of injection increasing the ignition delay. Retarding the timing after TDC results in lower ignition delay because of higher temperature and pressure, also the fact combustion happens in the expansion stroke reduces the maximum rate of heat release. From the figure, from -2° to 2° CA around TDC, $dQ/dt_{max}$ almost remains constant. Variation of CSL with respect to main timing is similar to the variation in $dQ/dt_{max}$.

Increase in rail pressure results in better atomization of the fuel and better mixing. Even though ignition delay decreases with increasing rail pressure, there is a relative increase in the pre-mixed charge at the end of ignition delay. This results in increase of the maximum rate of

pressure rise during the pre-mixed combustion stage and results in an increase of $dQ/dt_{max}$ and noise.

Increasing the pilot 1 quantity and pilot 2 quantity results in higher temperature and pressure due to the combustion of relatively higher fuel prior to main injection. This reduces the ignition delay of the cycle and results in lower rate of pressure rise during pre-mixed combustion and results in reduction of $dQ/dt_{max}$

So, based on the above discussions and analysis, $dQ/dt_{max}$ was selected for further validation in acoustic chassis dynamometer even though the value of linear correlation co-efficient was less. So the parameters that are included in the Rapid Control Prototyping system are given in the following table.

Table 4. Implemented parameters

| Parameters | Explanation |
|---|---|
| $\alpha_{x10}$, $\alpha_{x50}$ | Location of 10 % MFB and location of 50 % MFB |
| $dP/dt_{max}$ | Max. pressure gradient (with respect to time), location of maximum pressure gradient |
| $P_{max}$ | Max. pressure |
| $dQ/dt_{max}$ | Max. of rate of heat release (with respect and time) |
| $dQ/dt_{max\_filtered}$ | Max. of rate of heat release (with respect and time), End of combustion limited to 420° |
| $t_i$ | Ignition delay ($\alpha_{x10}$ – SOI) |
| $(dp/dt_{max})/t_i$ | Parameter combining max. pressure gradient and ignition delay. Ratio of max. pressure gradient and ignition delay. |
| CNL | Combustion Noise Level |

## *6.3 Validation tests*

Validation tests done on acoustic chassis dynamometer including microphone measurements are

- Acceleration tests

- Idle – Parameter sweeps
- 2000 rpm 6 bar BMEP – Parameter sweeps
- Controller trials

Two sets of Injector ETQ maps were tested simulating the drift in injectors. The base map is mentioned as reference ETQ and the new ETQ map which gives similar performance of drifted injector was named as offset ETQ. The pulse values were offset by 40% of its original value in the offset ETQ configuration.

### *6.3.1 Acceleration tests*

Three different types of accelerations were tested. They are

- LTI – Low Tip in – Slow rate of acceleration.
- MTI – Medium Tip in – Medium rate of acceleration.
- FTI – Full Tip in – High rate of acceleration.

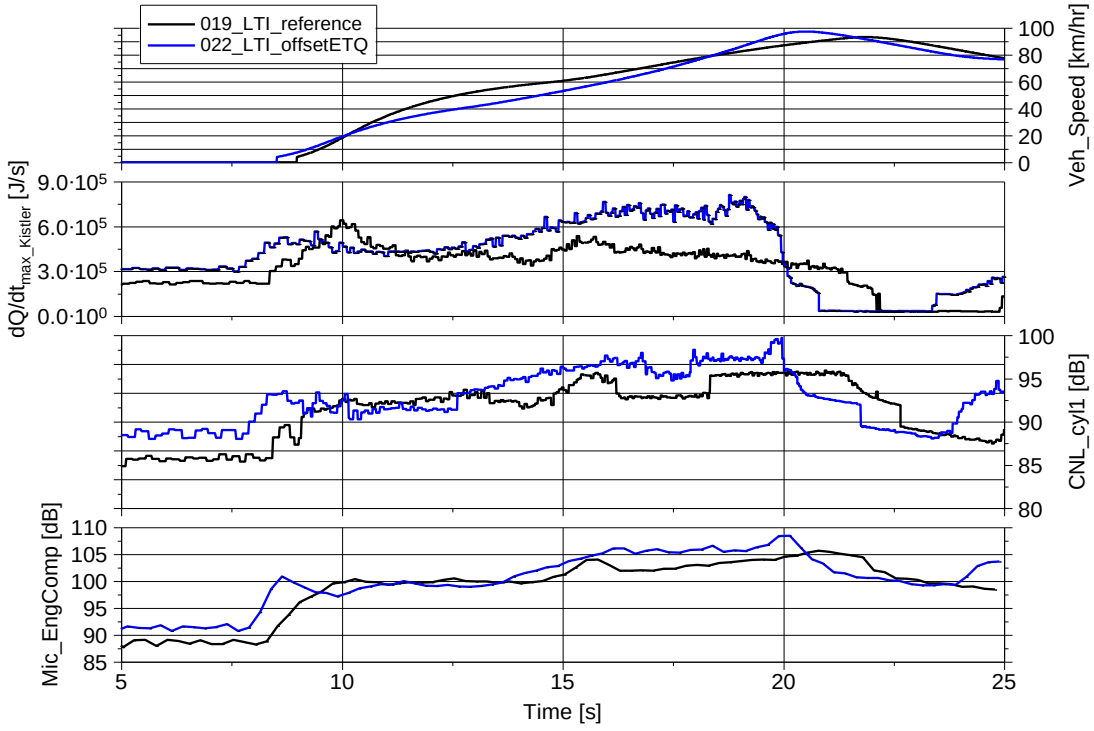


Figure 24. $dQ/dt_{max}$ and measured noise during slow rate of acceleration

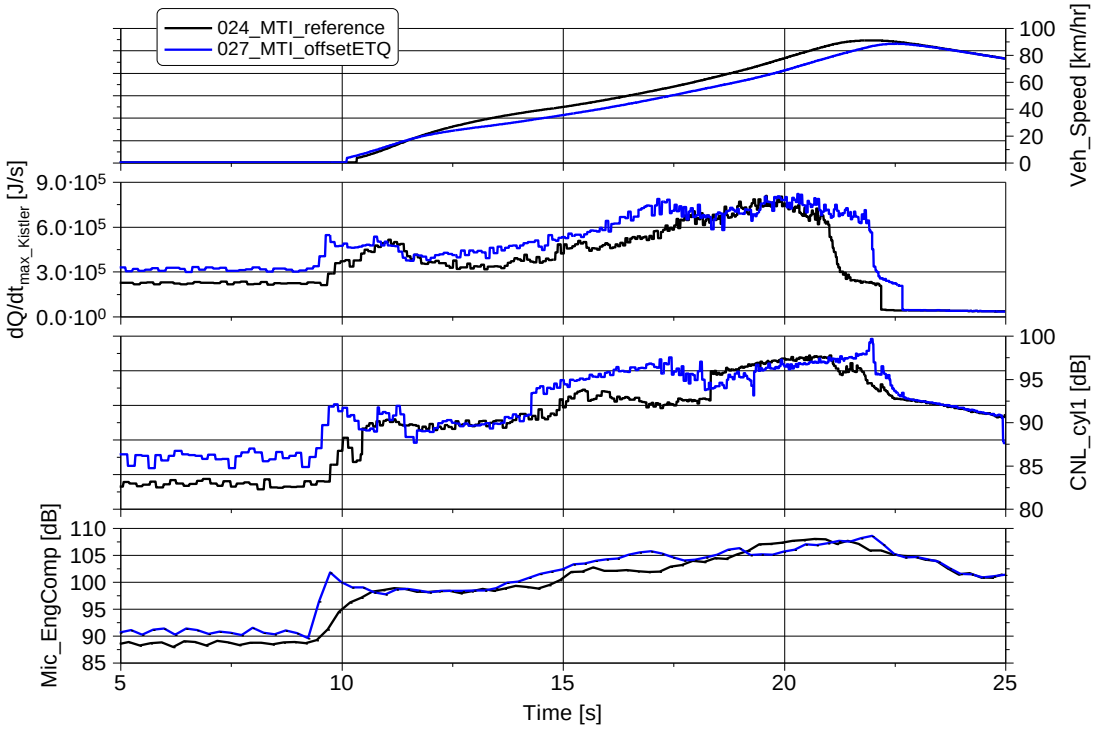


Figure 25. $dQ/dt_{max}$ and measured noise during medium rate of acceleration

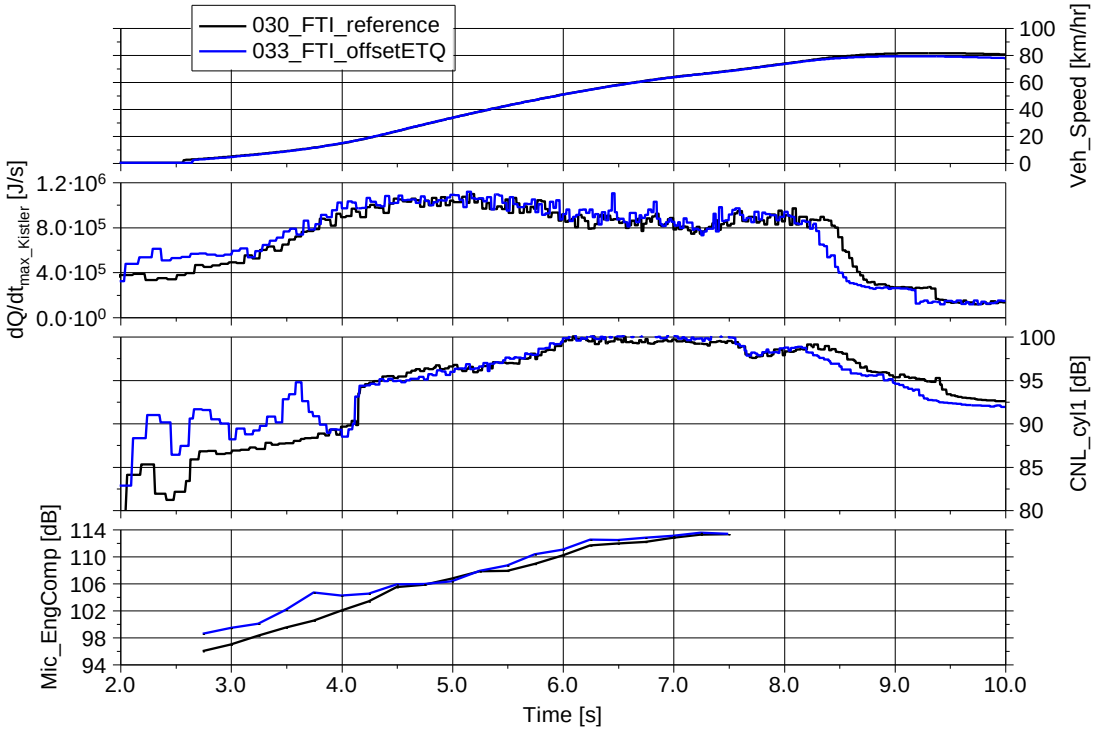


Figure 26. $dQ/dt_{max}$ and measured noise during high rate of acceleration

The above figures show the variation of microphone measurement and maximum rate of heat release and the calculated CNL for various rates of acceleration. Vehicle speed data is also plotted in the graph to compare the rate of pressing the accelerator pedal.

In all the three varying rates of acceleration test, microphone measurement correlates with the increase or decrease in dQ/dtmax. Maximum rate of heat release predicts the increase in noise with increasing acceleration even though relative level varies.

### *6.3.2 2000 rpm 6 bar BMEP tests*

The below figures shows the plots obtained at the acoustic chassis dynamometer,the values plotted here are the averaged values over time at the respective sweep point. Value of $dQ/dt_{max}$ for both the sensors, microphone measurement inside engine compartment and CNL wth the reference and offset ETQ maps at 2000 rpm and 6 bar BMEP.

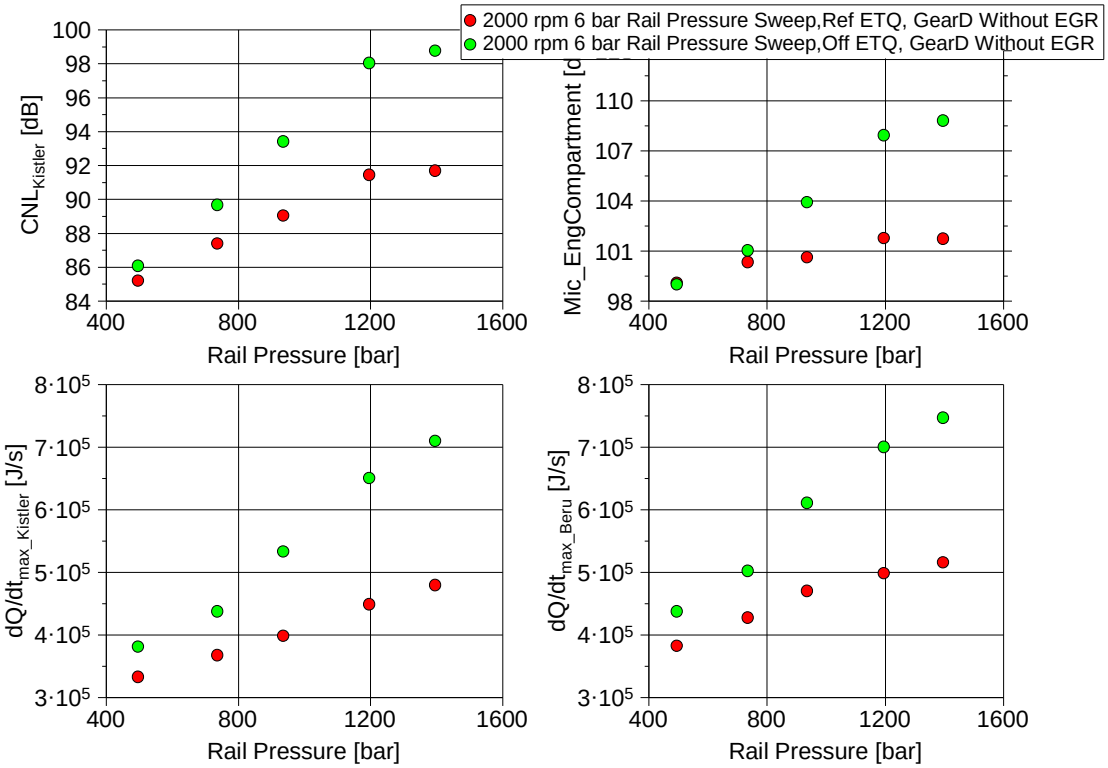


Figure 27. 2000 rpm 6 bar BMEP $dQ/dt_{max}$ and measured noise during rail pressure sweep

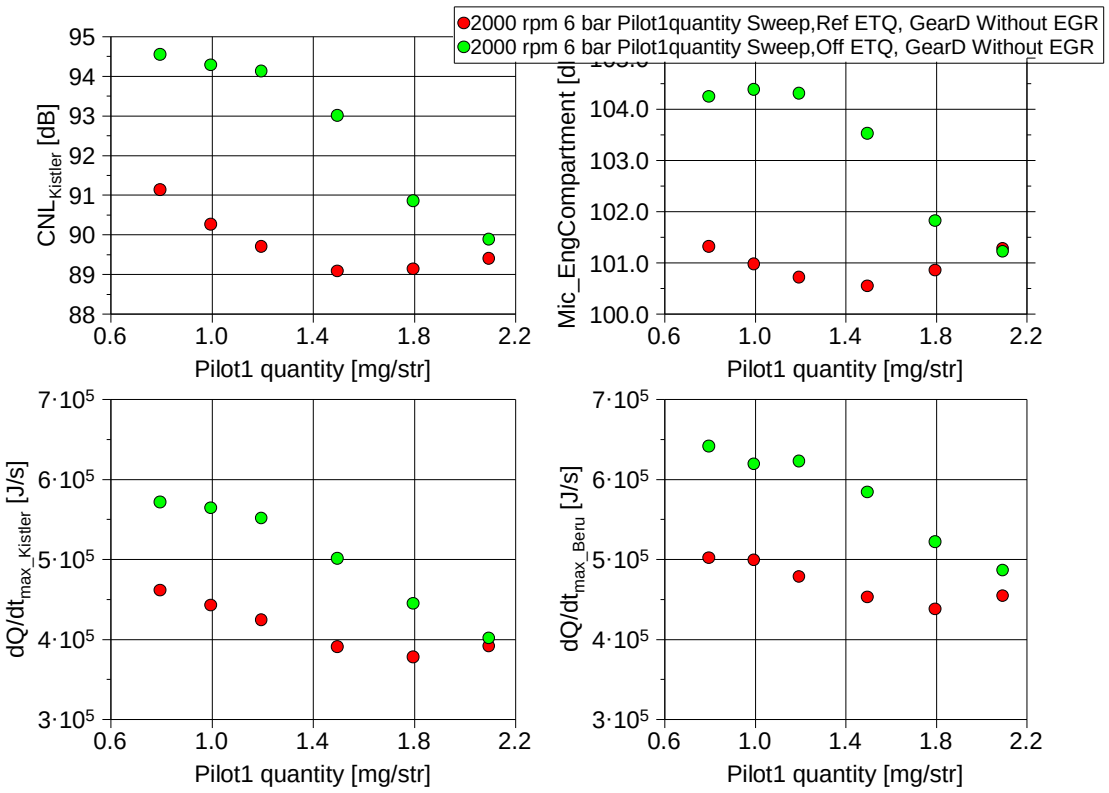


Figure 28. 2000 rpm 6 bar BMEP $dQ/dt_{max}$ and measured noise during pilot 1 quantity sweep

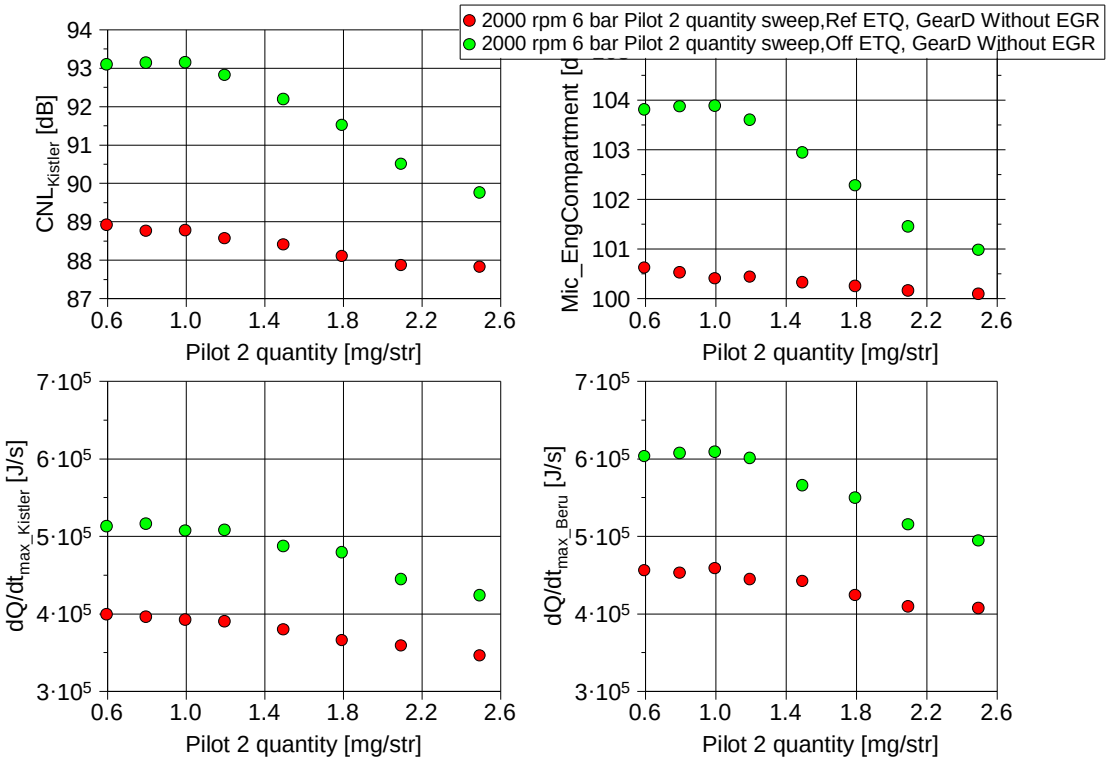


Figure 29. 2000 rpm 6 bar BMEP $dQ/dt_{max}$ and measured noise during pilot 2 quantity sweep

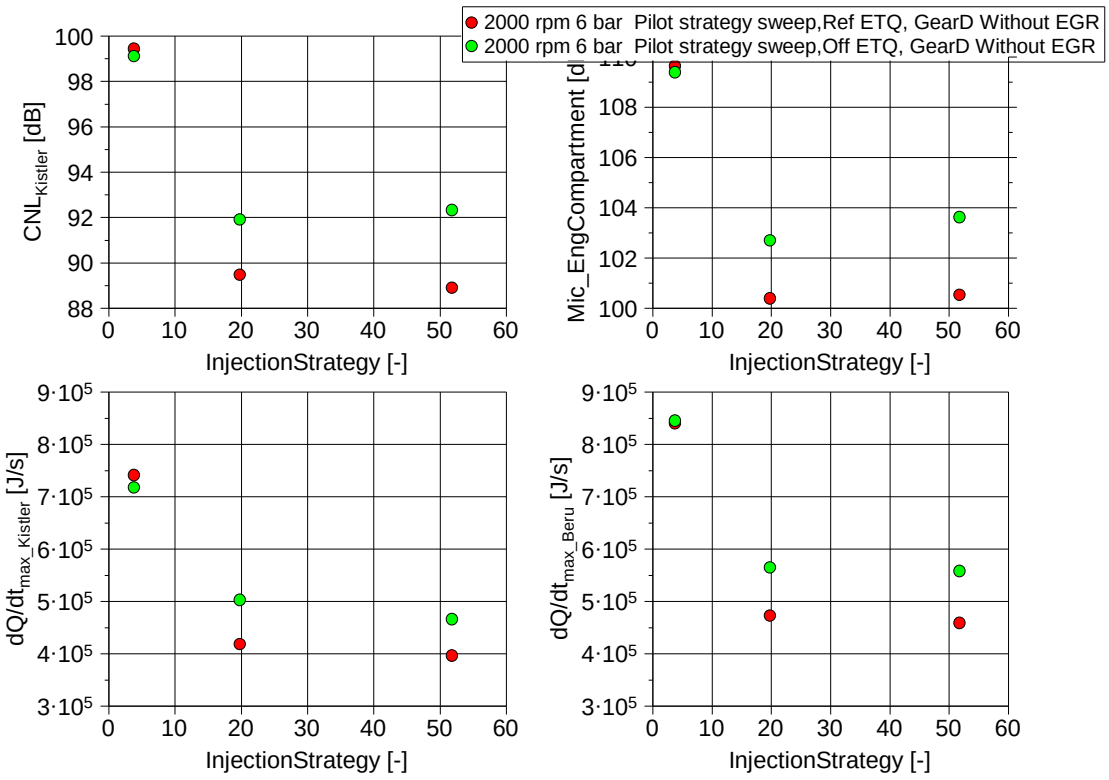


Figure 30. 2000 rpm 6 bar BMEP $dQ/dt_{max}$ and measured noise during pilot strategy sweep

In the figure 5.20, according to BOSCH naming convention, 4 in the x-axis represents only main injection, 20 represents main injection with single pilot injection, 52 represents main injection with 2 pilot injections.

During rail pressure sweep, there is a clear correlation trend between the measured microphone data and the $dQ/dt_{max}$ value. Increasing the rail pressure results in increased noise and increase in $dQ/dt_{max}$ value with both reference and offset ETQ map. At 500 bar rail pressure which is less than the optimum rail pressure at 2000 rpm 6 bar BMEP, there is a light increase in $dQ/dt_{max}$ value with the reference ETQ with no appreciable change in noise.

Noise and $dQ/dt_{max}$ decreases with increase in pilot 1 quantity. With reference ETQ after 1.6 mg/str of pilot quantity there is an increase in noise, which is detected by the increase in $dQ/dt_{max}$ value. With offset ETQ, there is no change in noise and $dQ/dt_{max}$ during initial sweeps indicating no pilot quantities. Noise and $dQ/dt_{max}$ continues to decrease with increase in pilot 1 quantity.

With Pilot 2 quantity there is no appreciable change in noise and $dQ/dt_{max}$ value from 0.6 to 1.2 mg/str. After 1.2 mg/str there is a small decrease in the noise with increase in pilot 2

quantity. With offset ETQ, the decrease in noise rate is higher, since the fuelling was higher. $dQ/dt_{max}$ value matches well with the measured microphone values.

With variation in number of pilot injections, no appreciable change when pilot injection strategy was reduced from 2 pilot injections to 1 pilot injection, but there is an increase in the noise and $dQ/dt_{max}$ value when both the pilot injections were cut-off.

### *6.3.3 Idle tests*

Similar to the sweeps at 2000rpm , 6bar BMEP, Sweeps were also performed at idle conditions.The vehicle was equipped with an automatic gear box and the tests were carried out in driving gear (Gear D) and with EGR on condition. the values plotted here are the averaged values over time at the respective sweep point.

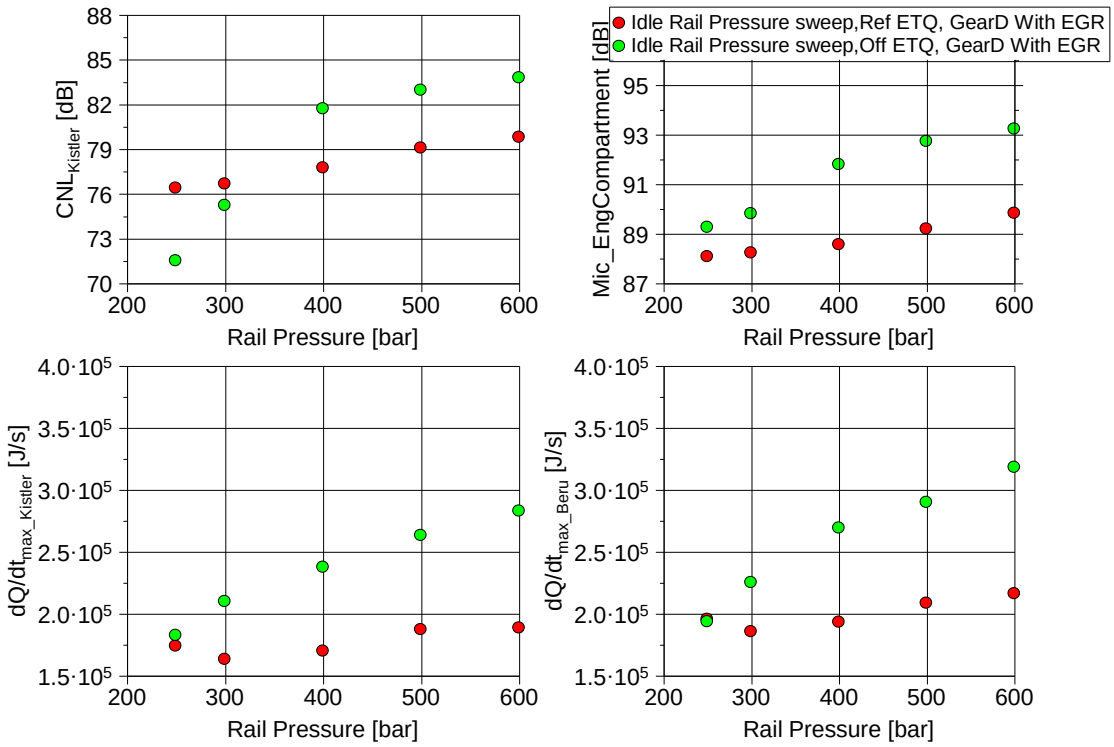


Figure 31. Idle $dQ/dt_{max}$ and measured noise during rail pressure sweep

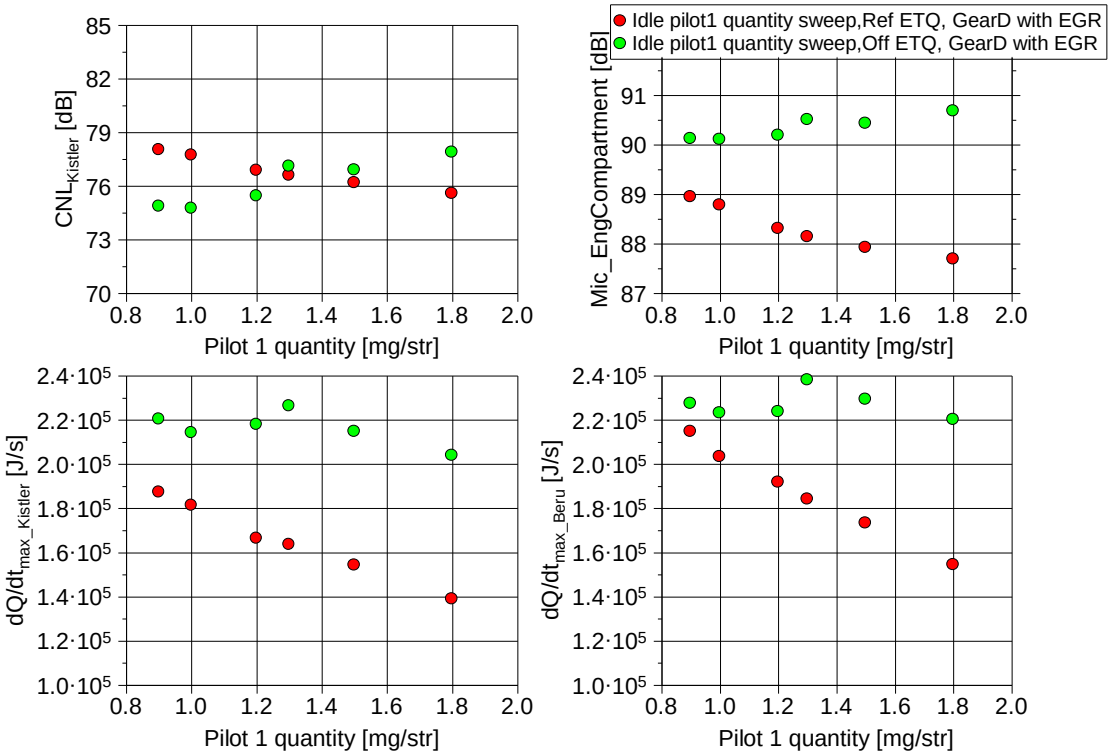


Figure 32. Idle $dQ/dt_{max}$ and measured noise during pilot 1 quantity sweep

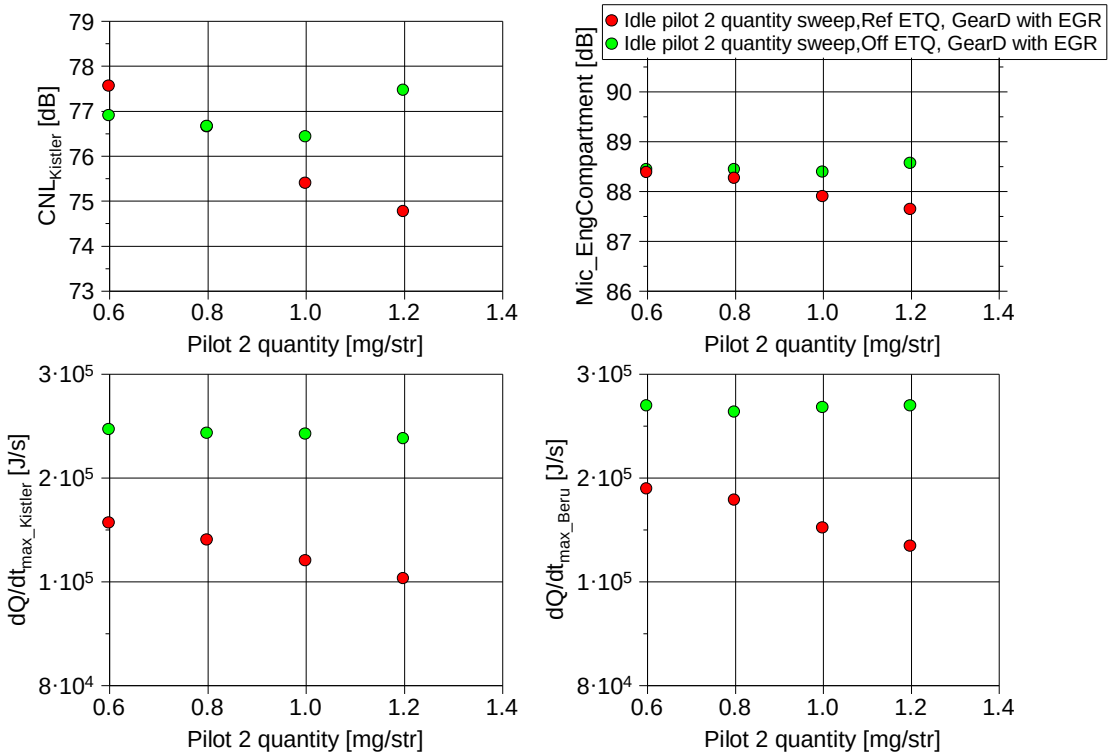


Figure 33. Idle $dQ/dt_{max}$ and measured noise during pilot 2 quantity sweep

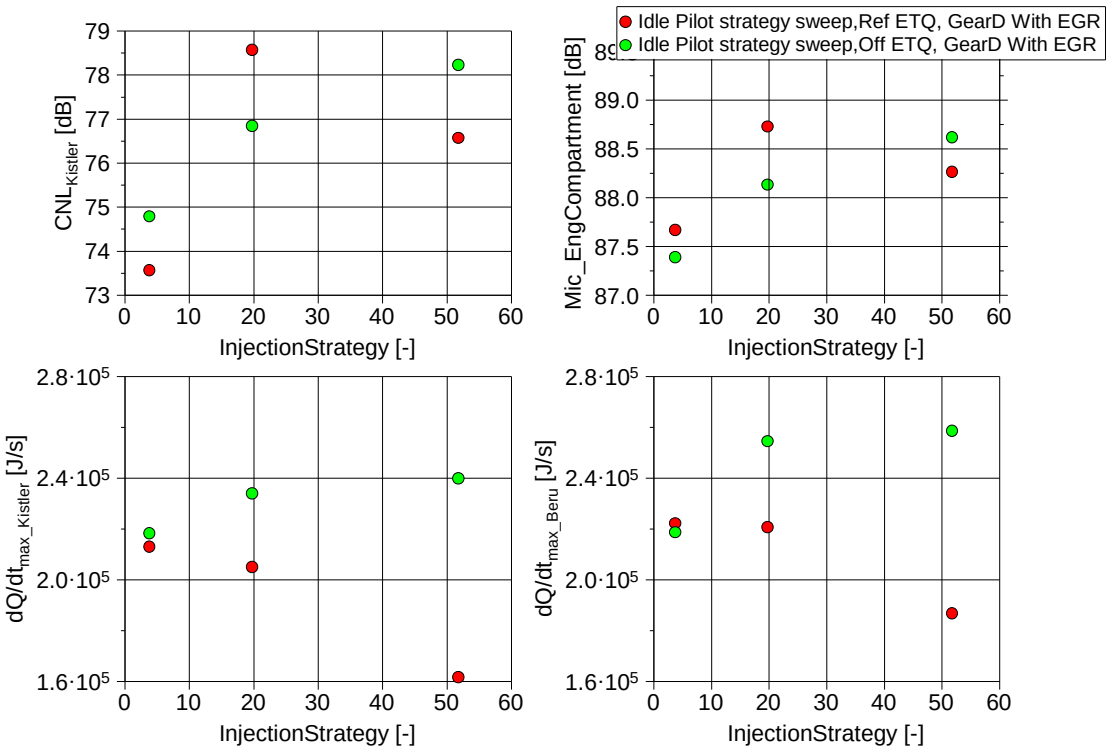


Figure 34. Idle $dQ/dt_{max}$ and measured noise during pilot strategy sweep

Increase in rail pressure results in increase in the noise measured with the offset ETQ.There is a similar increase in $dQ/dt_{max}$ value for increasing rail pressure with the reference ETQ. With the referencet ETQ, there is no increase in noise when the rail pressure is increased from 230 bar to 400 bar after 400 bar increase in rail pressure results in increase in the measured noise value. Similar trends were observed with $dQ/dt_{max}$ value.

During pilot 1 quantity sweep, there is a decreasing trend in the measured noise with increase in pilot 1 quantity with the reference ETQ. $dQ/dt_{max}$ value also decreases with increasing pilot 1 quantity for the reference ETQ. With offset ETQ there is no change in the measured noise and $dQ/dt_{max}$ value when the pilot 1 quantity is varied from 0.8 mg/str to 1.2 mg/str. After that there is a decrease in the noise and $dQ/dt_{max}$ value for increasing pilot 1 quantity.

With increase in pilot 2 quantity, there is a decrease in measured noise for both measured noise and $dQ/dt_{max}$ value with reference ETQ. With offset ETQ, there is no change in both measured noise and $dQ/dt_{max}$ value for increasing pilot 2 quantities indicating no change in the pilot 2 quantities with reference ETQ calibration.

When the number of pilot injections was varied, there is an increase in noise when the pilot injection strategy was reduced from 2 pilot injections to 1 pilot injection with the reference

ETQ, there is no considerable change with the offset ETQ.But when both the pilot injections were cut, there is a decrease in the measured noise.

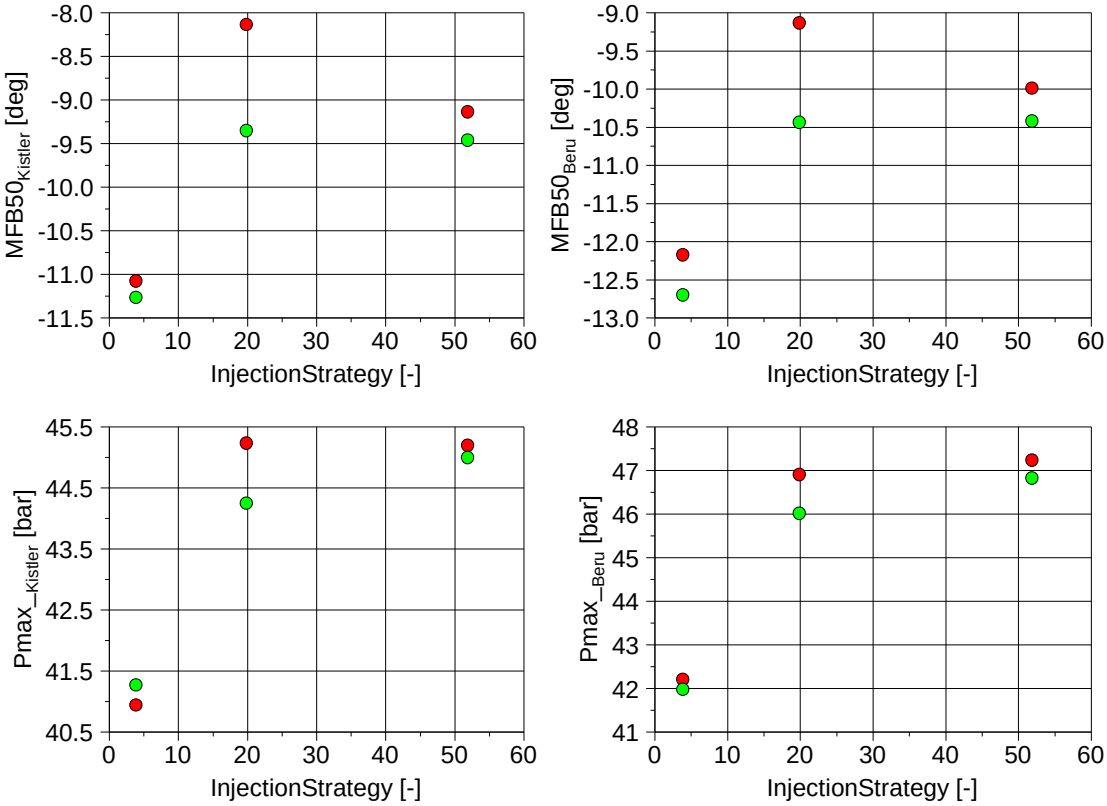


Figure 35. Idle $dQ/dt_{max}$ and measured noise during pilot strategy sweep

The above figure shows the variation of 50% burned mass fraction and maximum pressure obtained inside the cylinder measured during variation of number of pilots. When both the pilot injections were cut off, an increase in noise was expected, but the 50% mass fraction burned occurs very late in the cycle, -11 deg crank angle after TDC in cylinder 1 for the reference ETQ indicating the combustion starts very late and occurs at slow rate. This results in low peak pressure attained in the cylinder resulting in low $dQ/dt_{max}$ and noise values.

The trend between reference and offset ETQ was different due to the difference in fuelling at low load and low speed, but it follows the similar trend as that of $dQ/dt_{max.}$

### *6.3.4 Controller trials*

A simple PI controller was implemented to control the combustion noise by controlling $dQ/dt_{max}$ by reducing using rail pressure. The trial was done to illustrate the controllability of $dQ/dt_{max}$.

Test is started with a constant set point of $dQ/dt_{max}$ and controller on with reference ETQ map, then after a while offset ETQ map is loaded and then again base reference ETQ map is loaded again.

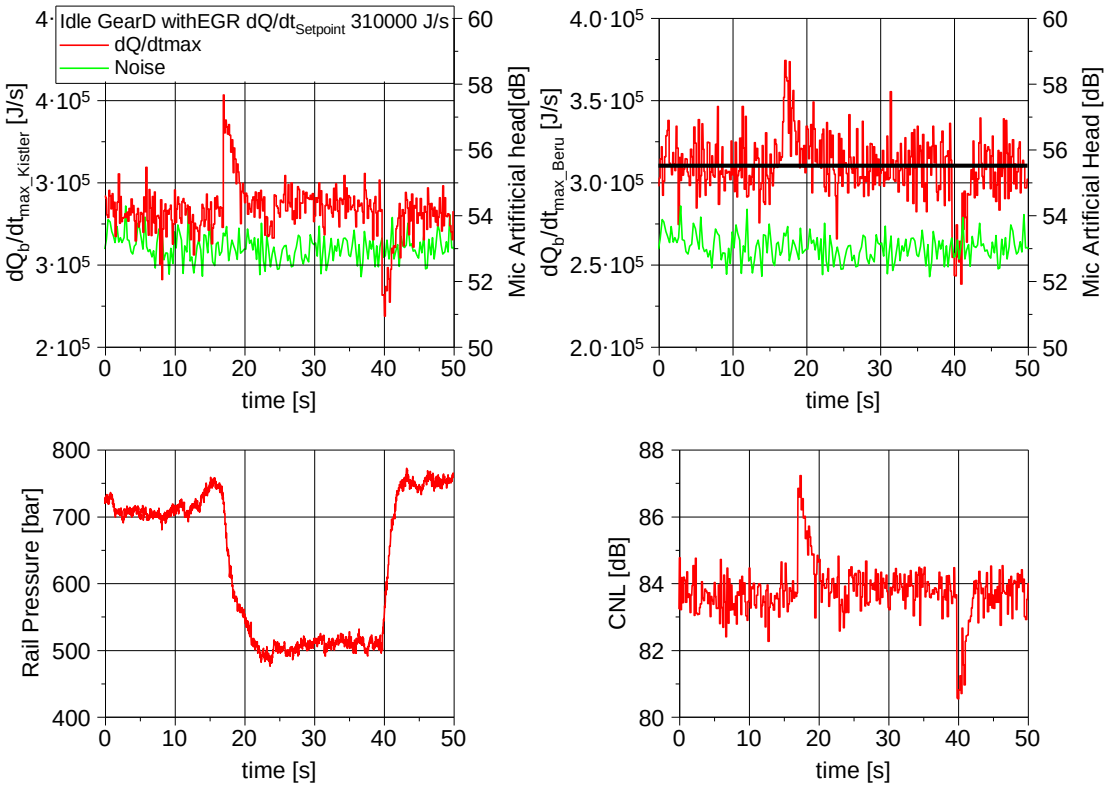


Figure 36. Controller trials reference-offset-reference ETQ

The above figure shows the $dQ/dt_{max}$ value and noise value with controller on.

The set point of $dQ/dt_{max}$ value was set to 310000 J/s and the test is started with reference ETQ map. When Offset ETQ map is flashed, because of higher fuelling there is an increase in $dQ/dt_{max}$ value and noise as expected. The controller reduces the rail pressure and keeps the noise level at the same level. The above test was carried out at idle Gear D with EGR.

# 7 CONCLUSIONS

*This chapter presents the conclusion drawn from the current study.*

The study infers that $dQ/dt_{max}$ correlates well with the reference combustion sound level at different operating conditions. The identified parameter $dQ/dt_{max}$ predicts the relative increase in noise at all the tested conditions even though the correlation efficiency between $dQ/dt_{max}$ and the reference CSL was very less at higher load and low loads, correlation efficiency increases when the engine is operated in the part load range. Figure 12 and table 1, shows that the parameter correlates to the combustion noise at different coolant temperature conditions (90deg C, 50 deg C and 30 deg C) and also with two different types of pressure sensor (Kistler and Beru).Table 2 shows that the parameter is simple to calculate in terms of computational power and it is easy to implement in real time systems.

$dQ/dt_{max}$ was incorporated in a Simulink real time interface model and was implemented in a Rapid Control Prototyping system (figure 40). Vehicle was fitted with cylinder pressure sensors and microphones and was fitted in an acoustic chassis dynamometer. Figure 9 & 10 shows the microphone locations. Only the microphone fitted inside the engine compartment recordings were compared with $dQ/dt_{max}$ for validation.

Validation test results (figure 24-35) shows that $dQ/dt_{max}$ relates well with the measured microphone noise using two different set of Injector energizing time maps. In Figure 36, Controller trials show that max rate of heat release can be used as a control parameter to control combustion noise at the tested conditions. The study also infers that the model used must be robust enough to identify and exclude the disturbances from the pressure sensors. Validation test results also show the accuracy of the parameter doesn't depends on the resolution of pressure sensor required, though higher resolution will increase the overall accuracy.

As a future work, tests should be performed to establish the relative correlation and limits between maximum heat release rate and noise. Further validation needs to be carried out at extreme climatic conditions and at higher altitude to establish the boundaries for controlling combustion noise using maximum rate of heat release rate. The above result is valid for the tested engine even though the initial calculation of Combustion Sound Level was carried out

with standard weighting functions. Application of this study to other type of engines must be verified, since the structure transfer function varies due to differences in construction.

# 8 REFERENCES


[1] Thomas Körfer, Thorsten Schnorbus et al “Integrated Diesel engine concept for lowest $CO_2$-emission requirements” , Aachener Kolloquium Fahrzeug- und Motorentechnik 2010

[2] Thorsten Schnorbus, Stefan Pischinger et al “Diesel combustion control with closed-loop control of the injection strategy”, SAE paper 2008-01-0651

[3] Thorsten Schnorbus, Dissertation “Ansätze für ein zylinderdruckgeführtes Einspritzmanagement beim Dieselmotor”, PhD.thesis

[4] Norbert Alt, Jack Nehl, et al “Combustion Sound prediction within combustion system development”, SIA “Vehicle Comfort” 200

[5] Stefan Heur, Dissertation “Verbrennungsgeräusch des direkteinspritzenden Hubkolbenmotors“

[6] FEV GmbH “CNL Calculation – Internal document”

[7] Stefan Pischinger, “Internal Combustion Engines”, Lecture Notes: Volume 1 & 2, Institute of Combustion Engines, RWTH, Aachen

[8] FEV GmbH “Closed loop combustion control – Internal document”

# APPENDIX A: SIMULINK MODEL

Parameters required for combustion analysis are included in the zero dimensional combustion model created using Simulink.

A zero dimension combustion model, which calculates the basic combustion parameters like IMEP, PMEP, Net IMEP and Mass fraction burned curves is incorporated with the selected noise parameters.

## *8.1 Zero dimension Combustion model*

Zero dimension Combustion model is a simple model of combustion system. It is called zero dimensional since no flow occurs in the system. It considers the condition in which no mass flow happens inside the system that is the condition at which the intake and exhaust valves were closed.

## *8.2 Mean effective pressure*

Mean effective pressure is calculated from the cylinder pressure data and cylinder volume. Pressure trace over the entire four strokes is multiplied by change in volume of the cylinder. Total summation of the product of pressure and change in volume over the four cycles divided by swept volume gives the IMEP. Summation of the product of pressure and change in volume over the compression and expansion stroke gives the net Indicated mean effective pressure of the engine. Difference between the IMEP and net IMEP gives PMEP.

$$\text{IMEP} = \frac{\sum_{0^\circ}^{720^\circ} \text{p.dV}}{\text{V}_\text{s}} \quad [1]$$

$$\text{Net IMEP} = \frac{\sum_{180^\circ}^{540^\circ} \text{p.dV}}{\text{V}_\text{s}} \quad [2]$$

$$\text{PMEP} = \text{IMEP} - \text{Net IMEP} \quad [3]$$

## *8.3 Start of combustion and end of combustion*

Many complex algorithms exist to determine the ignition delay and from that start of combustion are calculated. But in the current model, ignition delay is calculated as period

from start of Injection till 10% mass fraction burnt. Start of combustion is assumed at crank angle after which the injection happens. End of combustion is assumed as the crank angle at which the $PV^{\kappa}$ value reaches maximum in the expansion stroke. Heat release continues over the entire expansion stroke since some of the crevice volume fuel use to burn releasing some heat during the expansion stroke. The maximum value of $PV^{\kappa}$ for a $\kappa$ value of 1.15 gives a good prediction for the end of combustion. Since the expansion is assumed to polytropic, the above method gives a good indication for the end of combustion.

## 8.4 Heat release rate and mass fraction burned

Heat release rate is calculated using the first law of thermodynamics.

$$dQ = C_v m\, dT + p.\, dv \qquad [4]$$

Differentiating the ideal gas law gives,

$$mdT = \frac{V.dp + p.dV}{R} \qquad [5]$$

Substituting the equation [4.5] in [4.6] and using the relation $C_p - C_v = R$ and $C_p/C_v = \gamma$ ,we get

$$dQ = \left(\frac{1}{\gamma - 1}\right).V.\,dp + \left(\frac{1}{\gamma - 1}\right)p.\,dV \qquad [6]$$

Heat transfer to the walls and heat transfer due to crevice volumes are not considered in the heat release calculation approach.

Mass fraction burned is calculated using the heat release approach, individual sum of the heat release rate values gives the cumulative heat release rate. Normalized cumulative heat release values gives the mass fraction burned.

$$MFB(x\%) = \frac{\sum_{SOC}^{x\%\ burned} dQ}{\sum_{SOC}^{EOC} dQ} \qquad [7]$$

## 8.5 Pressure parameters

Peak cylinder pressure and location of maximum peak pressure are directly calculated from the cylinder pressure and crank angle trace. Maximum pressure gradient is calculated by

calculating the difference in pressure over the crank angle and then finding the maximum value of pressure gradient using maximum function in Simulink, also the crank angle at which the maximum pressure gradient occurs is also evaluated. By using the engine speed and the calculated maximum pressure gradient, pressure gradient with respect to time is calculated.

The combined parameters are calculated by using the peak pressure value, Ignition delay and the pressure gradient. The following figures show the representation of pressure parameters using an in cylinder pressure trace and the overview of the pressure parameter calculation block in Simulink

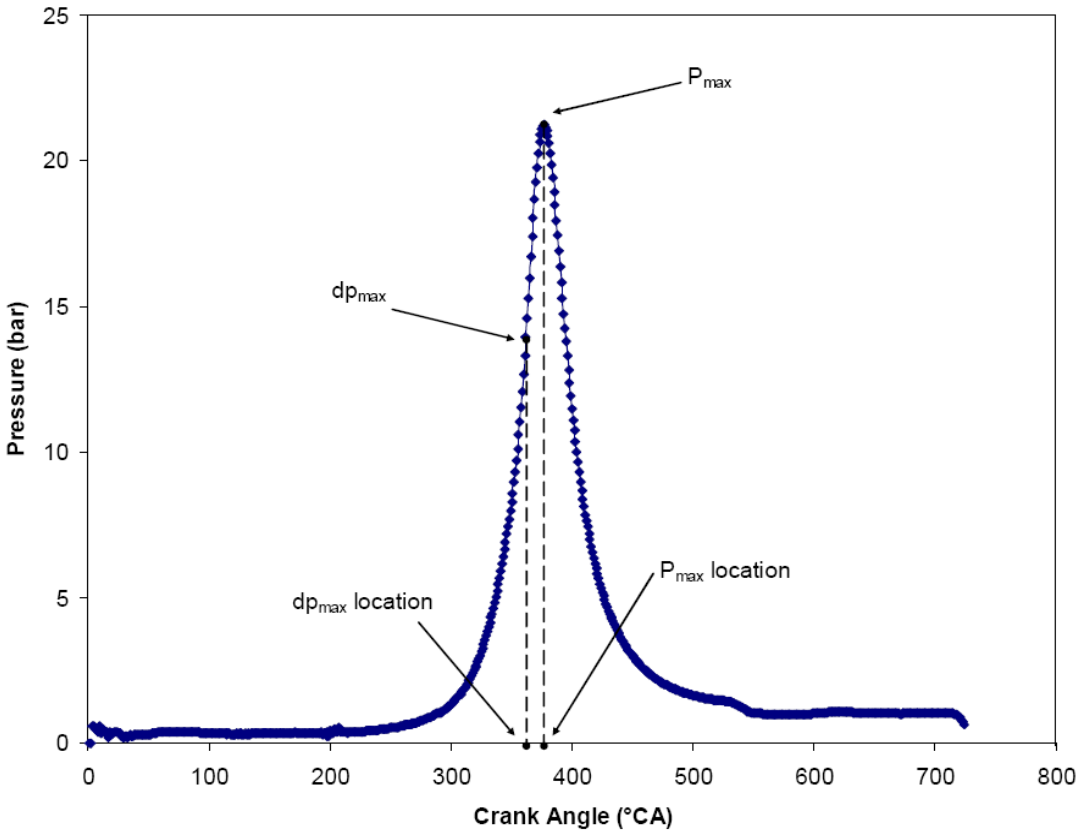


Figure 37. Cylinder pressure with pressure parameters

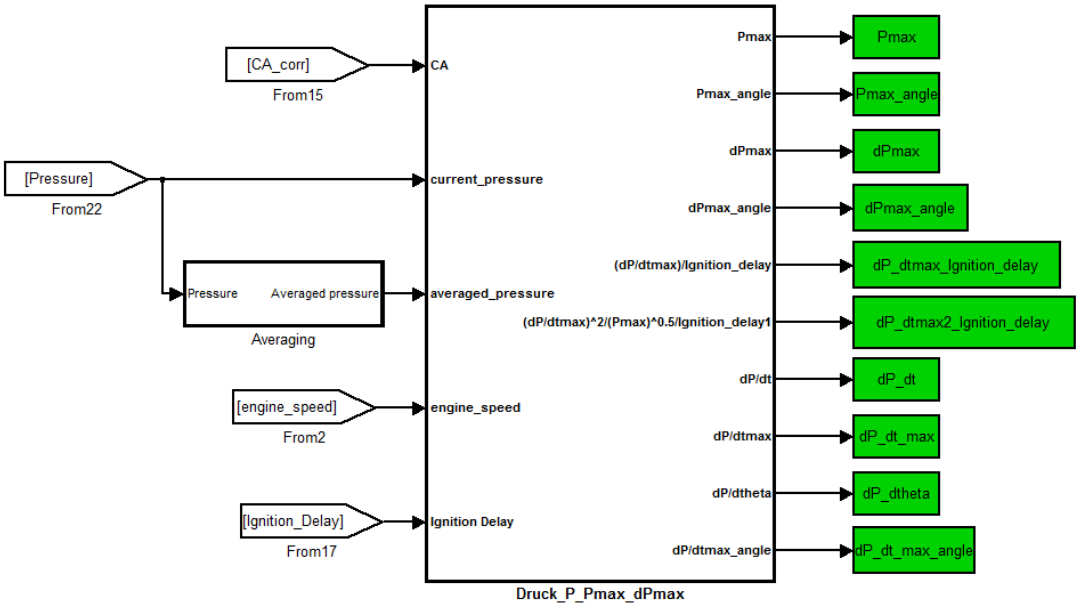


Figure 38. Overview of pressure parameters calculation block in Simulink

## 8.6 Combustion noise level

CNL is calculated in a separate block, in which the pressure data in time domain is converted to frequency domain by taking FFT of the pressure signal. Then the CNL block uses the A-weighting function and structure attenuation function to calculate CNL.

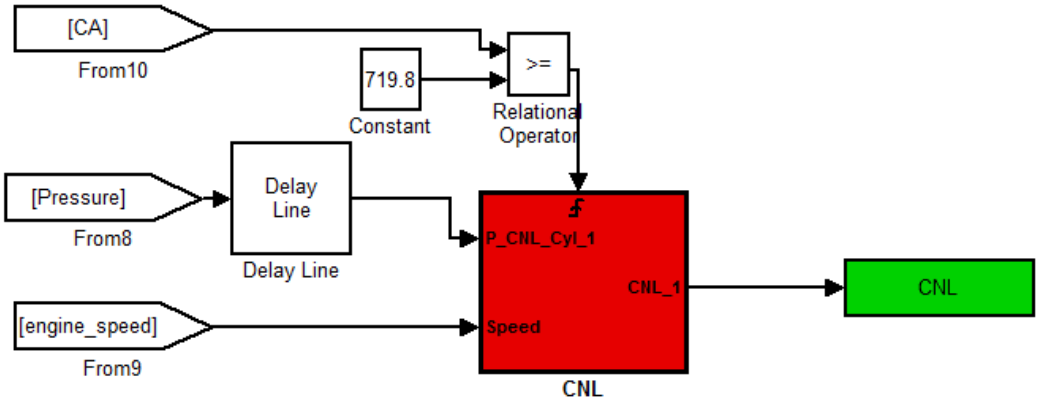


Figure 39. Combustion noise level calculation block in Simulink

## 8.7 Validation test setup

For validation test, the model is simplified with only relevant parameters that show reasonable correlation with CSL. This simplified model is incorporated in a RCP interface.

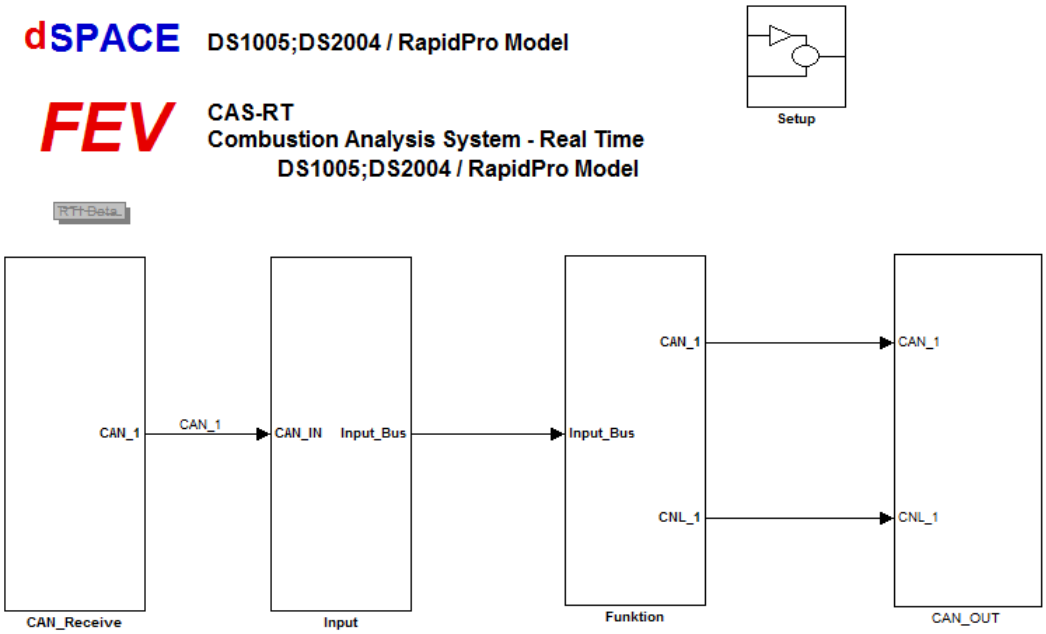


Figure 40. Overview of RCP interface model in Simulink

The above figure shows the overview of the real time interface model. “CAN_Receive” block receives input from various sensors fitted in the vehicle that are required for the model through CAN interface. Processing of the input signals such as Pressure pegging, Zero-point correction, unit conversions for different sensor data are done in the “Input” block. “Funktion” block contains the combustion analysis model that calculates the combustion parameters, pressure parameters and the output values that are required by the engine or other systems. “CAN_OUT” block contain the necessary blocks which process the output data given by the model and then send it through CAN. Additionally, CNL is also incorporated with the model and cylinder pressure signal from one of the cylinder was used for calculating combustion noise level. Since CNL calculation requires high computational power, only one cylinder pressure signal was post processed for calculating CNL.

# APPENDIX B: LOAD POINTS

Table 5. Load points

| Load point | | | | |
|---|---|---|---|---|
| N [rpm] | Bmep [bar] | | Coolant temperature [°C] | Number of pilot injections [-] |
| 790 | 1 | Idle | 90 | 2 |
| 1250 | 3 | | 90 | 2 |
| 1500 | 4 | | 90 | 2 |
| 1500 | 4 | | 90 | 1 |
| 1500 | 6 | | 90 | 2 |
| 1500 | 6 | | 90 | 1 |
| 2000 | 6 | | 90 | 2 |
| 2000 | 6 | | 90 | 1 |
| 2000 | 6 | | 90 | 0 |
| 2000 | 14 | | 90 | 1 |
| 2200 | 9 | | 90 | 1 |
| 820 | 1 | Idle | 50 | 2 |
| 1250 | 3 | | 50 | 2 |
| 1500 | 4 | | 50 | 2 |
| 1500 | 6 | | 50 | 2 |
| 2000 | 6 | | 50 | 2 |
| 2000 | 14 | | 50 | 1 |
| 2200 | 9 | | 50 | 1 |
| 900 | 1 | Idle | 30 | 2 |
| 1250 | 3 | | 30 | 2 |
| 1500 | 4 | | 30 | 2 |
| 1500 | 6 | | 30 | 2 |
| 2000 | 6 | | 30 | 2 |

# APPENDIX C: CYLNDER PRESSURE SENSORS

Two pressure sensors are installed in the engine.

- cylinder 1 –Kistler sensor - piezoelectric
- cylinder 2 –Beru sensor - piezoresistive

Piezoelectric effect is based on the property of quartz crystal to accumulate charge on one side, when it is subjected to stress on other side, the accumulated charge is directly proportional to the stress acting on it. So, when one side of the crystal is exposed to the cylinder pressure, the accumulated charge will give a direct indication of the cylinder pressure. A glow plug integrated piezoelectric pressure sensor was fitted in the cylinder 1.

The piezoresistive pressure sensor builds on the semiconductor. Under mechanical stress, the change in the electrical resistance of semiconductors is up to two orders of magnitude greater than in metals. This type of sensor therefore opened up completely new applications compared with the metal strain gage methods of the time. Since then, other similar techniques have been developed, such as thin film on metal and thick layer on ceramic. A glow plug integrated piezo resistive pressure sensor from Beru was attached to cylinder 2.

They both are connected to the ETAS unit, cam and crank sensor was also connected to the ETAS unit for calculating the crank angle data. The basic input data like coolant temperature, inlet air temperature, air mass, main and pilot injection quantities and timing, engine speed etc. are received by the ETAS system through CAN. ETAS system sends this data to the dSpace unit. The real time model is imported in the dSpace module and the model calculates the required parameters. dSpace unit then sends the calculated values back to the ETAS system and the control values to the Rapid Prototyping system. The model is calibrated according to the engine specification and the pressure sensors also were calibrated.